Remote Sensing Applications: Society and Environment 38 (2025) 101544

Contents lists available at ScienceDirect

Remote Sensing Applications: Society and Environment

journal homepage: www.elsevier.com/locate/rsase

Spatially explicit assessment of carbon storage and sequestration in forest ecosystems

Bruna Almeida [b,c,d,*], Luís Monteiro [b], Rafaela Tiengo [c,e], Artur Gil [c,f], Pedro Cabral [a,b,**]

[a] School of Remote Sensing and Geomatics Engineering, Nanjing University of Information Science and Technology, Nanjing 210044, China
[b] NOVA Information Management School (NOVA IMS), Universidade Nova de Lisboa, Campus de Campolide, 1070-312 Lisboa, Portugal
[c] Centre for Ecology, Evolution and Environmental Changes (cE3c), Azorean Biodiversity Group (GBA), University of the Azores (UAc), Faculty of Sciences and Technology (FCT-UAc), Rua Mãe de Deus, Campus Universitário de Ponta Delgada, Edifício Do Complexo Científico, 9500-321, Ponta Delgada, Portugal
[d] Potsdam Institute for Climate Impact Research (PIK), Member of the Leibniz Association, P.O. Box 6012 03, D-14412 Potsdam Germany
[e] Departamento de Ingeniería y Gestión Forestal y Ambiental, ETSIMFMN, Universidad Politécnica de Madrid, 28040 Madrid, Spain
[f] IVAR—Research Institute for Volcanology and Risk Assessment, University of the Azores, 9500-321 Ponta Delgada, Portugal

ARTICLE INFO

Keywords:
Climate regulation
Vegetation dynamics
Sustainable development goals
Geographical information systems
Machine learning

ABSTRACT

Forests play an important role in the global carbon cycle, making accurate assessments of carbon dynamics essential for effective forest management and climate change mitigation strategies. This research examines the spatiotemporal patterns of carbon storage and sequestration (CSS) in forests' aboveground biomass using satellite data, machine learning (Support Vector Machines), carbon modelling and spatial statistics. The methodology follows a two-step classification process: (i) binary forest classification and (ii) forest type classification, mapping seven forest types within two main categories - Broadleaves (*Quercus suber, Quercus ilex, Eucalyptus* sp., and other species) and Coniferous (*Pinus pinaster, Pinus pinea,* and other species). We analyzed the relationship between forest type and CSS at the Nomenclature of Territorial Units for Statistics (NUTS) III level and identified spatial clusters, outliers, and hot and cold spots of carbon sequestration at the municipal level across mainland Portugal. The broadleaved category demonstrated the highest classification accuracy in both years, decreasing slightly from 90.3 % in 2018 to 89 % in 2022, while the Coniferous group had the lowest accuracy, declining from 84.1 % in 2018 to 83.6 % in 2022. Anselin's Local Moran's I identified clusters of carbon sequestration, while the Getis-Ord Gi analysis confirmed these findings, revealing statistically significant hotspots of carbon sequestration in the northern and central regions and cold spots in the southern region. By providing insights at the sub-regional and municipal levels, this study offers a robust framework to support sustainable forest management and climate change mitigation strategies. Moreover, it can assist decision-makers in prioritizing natural capital, and developing nature-based solutions to tackle climate change and biodiversity loss.

* Corresponding author. NOVA Information Management School (NOVA IMS), Universidade Nova de Lisboa, Campus de Campolide, 1070-312 Lisboa, Portugal.
** Corresponding author. NOVA Information Management School (NOVA IMS), Universidade Nova de Lisboa, Campus de Campolide, 1070-312 Lisboa, Portugal.
E-mail addresses: balmeida@novaims.unl.pt (B. Almeida), cabral@nuist.edu.cn (P. Cabral).

https://doi.org/10.1016/j.rsase.2025.101544
Received 31 October 2024; Received in revised form 6 April 2025; Accepted 8 April 2025
Available online 9 April 2025

1. Introduction

Forest carbon pools are increasingly threatened by the conversion of forests to other land uses (Fedrigo et al., 2014; Fitts et al., 2021; M. Zhang et al., 2019). Carbon storage and sequestration (CSS), as one of many competing land uses, refers to the amount of carbon captured and stored within a given pool (Bui et al., 2018; Cunha et al., 2021; Goetz et al., 2009; Paul et al., 2022). Among carbon pools, aboveground biomass in a forest (AGB) is the most significant, accounting for approximately 50 % of a forest's carbon content, though the precise fraction may vary depending on species and environmental conditions (Cong et al., 2023; Houghton et al., 2009; Qasim and Csaplovics, 2023; Spawn et al., 2020).

Given the strong correlation between carbon stocks and land use types (King et al., 2024), there is a growing demand for mapping carbon sinks and sources (Jiang et al., 2022), identifying opportunities for land use conversion (Han et al., 2022), and understanding the factors that influence carbon dynamics (Keith et al., 2021a). These knowledge gaps are particularly relevant in the context of major international commitments, including the Kyoto Protocol, the Paris Agreement, and the United Nations Sustainable Development Goal 15 (SDG 15). Notably, SDG 15 emphasizes the reduction of lowering greenhouse gas emissions (GHG) and the mitigation of climate change through the preservation, restoration, and sustainable management of terrestrial ecosystems (United Nations, 2023).

Cutting-edge remote sensing technologies provide a time- and cost-efficient method for estimating biophysical indicators of vegetation and surface conditions across broad temporal and spatial scales (J. Zhang et al., 2019). By leveraging these technologies, researchers can build long-term observational records (Li, 2023), enabling the extraction of ecologically meaningful information for large-scale monitoring (Holzwarth et al., 2020). Additionally, advancements in cloud-based computing, geoinformatics, and big spatiotemporal data analytics have expanded the toolkit available to researchers, as well as land and natural resource managers (Manley et al., 2022; Tiengo et al., 2024). For instance, Google Earth Engine (GEE) (Google, 2023) provides a cloud-based platform that allows users to access, process, and analyze large-scale satellite imagery and geospatial data (Gorelick et al., 2017). GEE facilitates the efficient retrieval, manipulation, and export of data from multiple sources, enabling the integration of satellite-derived indices, climatic data, and other environmental variables into carbon modelling workflows (Navarro, 2017; Pérez-Cutillas et al., 2023). These technologies can be integrated with a wide range of open-source software, such as those developed by Stanford University through the Natural Capital Project, to support spatially explicit modelling of natural and urban ecosystems (Natural Capital Project, 2023). By leveraging these advancements, studies can achieve higher precision and scalability in monitoring spatiotemporal patterns of CSS, offering valuable insights for sustainable forest management and land-use planning. For modelling carbon in terrestrial ecosystems, the InVEST CSS model provides critical information on landscape carbon content and the changes in carbon storage over time (Lade et al., 2020; Nelson et al., 2009; Polasky et al., 2011). Several studies have applied the InVEST CSS model to assess forest carbon pool dynamics (Han et al., 2022; Hudak et al., 2020; Islam et al., 2022; Matsala et al., 2020; Meddens et al., 2022) and to evaluate how different land uses and management strategies contribute to the conservation of carbon-rich ecosystems (Hossain and Hashim, 2019; Islam et al., 2022; Y. Li et al., 2024; Rogers et al., 2019). Similarly, research has emphasized the need for further investigation into spatial patterns and relationships between carbon estimates and terrestrial biomes (Nowak et al., 2022; Pan et al., 2023), the links between tree species and carbon sequestration (Narine et al., 2019), carbon trade-offs associated with land conversion (Ermitão et al., 2023), and the key drivers influencing carbon stocks (Chen et al., 2020; H. Li et al., 2024; Naidoo et al., 2019).

To address these gaps, the objectives of this study are: (i) classify forest and non-forest ecosystems, including the differentiation of specific forest types through binary and multiclass classification techniques, (ii) estimate CSS in AGB of forests in Portugal over a five-year interval (2018–2022), (iii) analyze the relationship between forest types and potential carbon sequestration, and (iv) identify hot and cold spots of forest carbon distribution at sub-regional (NUTS III) and municipal levels. Additionally, the study evaluates Portugal's progress toward sustainable development by assessing two of the five SDG 15.2.1 indicators: 1) forest extent and change rates and 2) AGB stock.

The methodology is structured into three main components. The first part involves a two-step classification process implemented in GEE. This includes a binary classification of forest and non-forest areas, followed by a multiclass classification that differentiates forest types using the Support Vector Machines (SVM) algorithm (Boser et al., 1992), along with hyperparameter tuning and accuracy assessments. The second component focuses on quantifying CSS in forest ecosystems using the InVEST CSS model. The third component applies Exploratory Spatial Data Analysis (ESDA) tools in ArcGIS Pro (ESRI, 2023) to detect statistically significant local clusters, outliers, and hot and cold spots of carbon sequestration using Anselin's Local Moran's I statistic (Anselin, 1995), the Getis-Ord Gi statistic (Getis and Ord, 1992) and the Global Moran's I statistic (Moran, 1950). The results are analyzed at NUTS III and municipal levels, capturing the spatial patterns of CSS in relation to forest type distribution.

This research is particularly relevant for countries like Portugal, which face significant challenges, including an aging population and persistent shortcomings in land and forest management (Santos et al., 2023b). With over 90 % of forests under private ownership, there is an urgent need for informed, strategic decision-making to ensure sustainable management practices (Cunha et al., 2021). A recent study by David et al. (2024), which maps ecosystem services (ES) in Portugal and integrates them into the ASEBIO index, underscores this urgency by revealing a 28-year gap between modeled and stakeholder-perceived ES potential.

By analyzing the spatiotemporal patterns of CSS in forests, this research provides actionable insights for sustainable land-use planning and forest management. Moreover, this study supports broader SDG 15 objectives by identifying carbon hotspots at sub-regional and municipal levels, fostering a deeper understanding of forest composition and functionality. Beyond evaluating CSS, the findings highlight the role of specific tree species as key contributors to carbon sinks, while spatial patterns reveal areas of carbon gain and loss, offering valuable information for climate change mitigation strategies. These insights enhance our understanding of terrestrial ecosystems mapping, addressing critical challenges such as deforestation, monoculture dominance, and rural land

abandonment. Furthermore, this approach can be integrated into decision-making processes, aiding policymakers in prioritizing natural capital and developing nature-based solutions to combat climate change and biodiversity loss.

2. Material and methods

2.1. Study area

The area of interest is mainland Portugal (Fig. 1), located in southwestern Europe, covering approximately 90,000 km^2 of the Iberian Peninsula. The territory is administratively divided into 23 NUTS III subregions and 278 municipalities.

Portugal's climate is characterized by a Mediterranean regime with distinct regional variations influenced by latitude, proximity to the Atlantic Ocean, and topography. The northern regions experience cooler and wetter conditions, with average annual precipitation exceeding 1200 mm, whereas the southern regions are drier and warmer, often receiving less than 600 mm annually (Coelho et al., 2013). Summers are typically hot and dry across the country, while winters are mild with occasional rainfall. These climatic gradients significantly impact forest composition, growth rates, and carbon sequestration potential.

At the national scale, forest ecosystems dominated by Cork and Holm oak, Pine trees, and *Eucalyptus* sp. Represent a crucial natural resource, covering approximately 34 % of the country's territory (Eurostat, 2023). These forests provide a diverse array of non-wood forest products, such as cork, pinecones, nuts, and resins, which play a significant role in the national economy (FAO - UN, 2020). The flat terrain of the southern regions supports extensive agriculture and agroforestry systems, characterized by low-density evergreen oak species such as Cork oak and Holm oak (Santos et al., 2023a). In contrast, the northern region is marked by a higher concentration of small landholdings, family agriculture, and forests of Pine and *Eucalyptus* sp. (Wentling et al., 2021).

Every year, vast portions of forests are lost due to wildfires, directly impacting public health, local communities, and industries reliant on forestry-related activities such as cork and timber production (Ermitão et al., 2023). The country faces increasing deforestation and land degradation driven by climatic change, evolving land-use patterns, and socio-economic factors (Sil et al., 2017). The summer of 2017, for instance, was marked by catastrophic fires in Pedrógão Grande and other regions, resulting in 66 fatalities and widespread devastation (Ramos et al., 2023). The prevalence of *Eucalyptus* monocultures and abandonment of traditional land management practices have heightened fire risks, while hotter summers and prolonged fire seasons exacerbate the problem (Fonseca et al., 2019). These wildfires disrupt biodiversity and essential ES such as climate regulation, habitat and genetic resources (Cong et al., 2023), releasing substantial amounts of CO_2 into the atmosphere and compromising CSS (Paul et al., 2022). The decline of rural activities and widespread land abandonment have further aggravated this issue, leading to unmanaged, homogeneous forest landscapes that are highly vulnerable to wildfires and other disturbances (Cunha et al., 2021). These challenges are exacerbated by demographic imbalances, with large population centers concentrated along the coast, leaving inland regions sparsely populated and underdeveloped (Araya and Cabral, 2010).

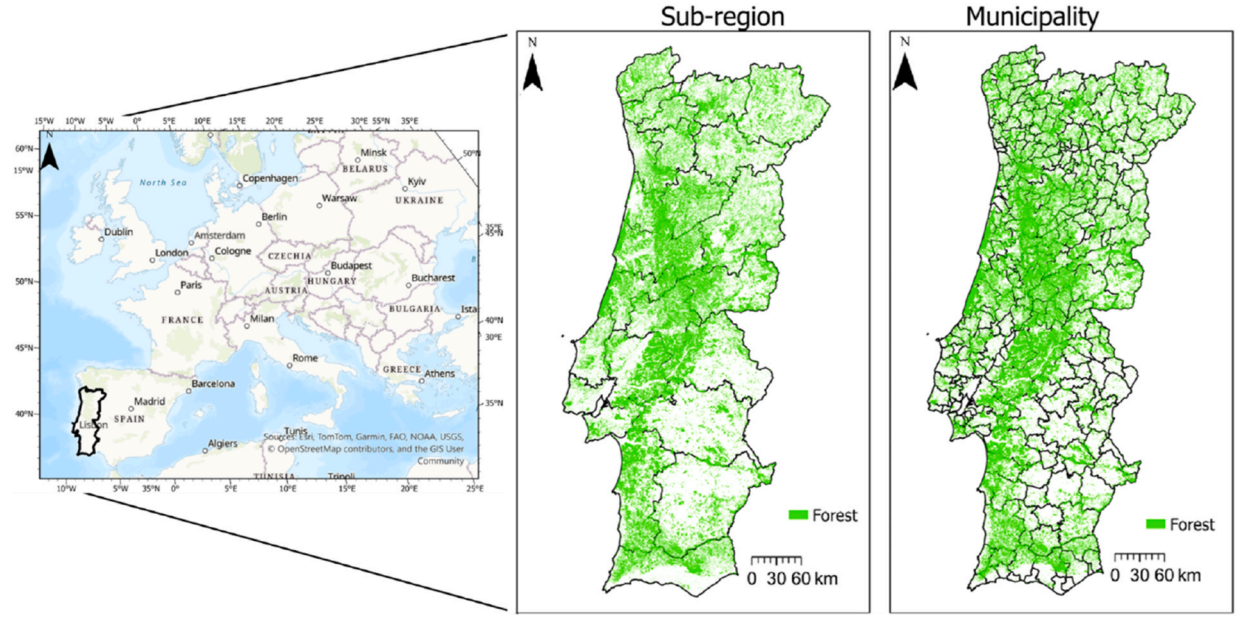

Fig. 1. Study area within Europe and the distribution of national forests in 2018 across subregions - NUTS III (Nomenclature of Territorial Units for Statistics) and municipalities. Refer to the Supplementary Materials to have further details on NUTS III and municipality codes and names.

2.2. Methods

Fig. 2 summarizes the methodological process, which begins with data acquisition and processing in GEE. This platform not only provides most of the required datasets but also offers powerful computational capabilities (Kumar and Mutanga, 2018; Navarro., 2017; Tiengo et al., 2021). The processed outputs are then integrated into the InVEST CSS model to estimate CSS in AGB at the national, sub-regional, and municipal levels. Finally, spatial statistical analyses are conducted to identify hot and cold spots of forest carbon distribution.

2.2.1. Data

This study utilizes Sentinel-2 imagery, known for its high spatial resolution (10 m) and frequent revisit time (5 days), to map forest types across Portugal for the years 2018 and 2022. Satellite data acquisition and processing were conducted using GEE platform, selecting images with cloud cover below 10 % and computing a median value from all valid observations. To constructed the data stack, all available spectral bands were considered, except those related to atmospheric effects (Bands 1, 9, and 10). Additionally, three spectral indices (Normalized Difference Vegetation Index (NDVI), Enhanced Vegetation Index (EVI), and Soil-Adjusted Vegetation Index (SAVI)) were included, along with slope and elevation data. NDVI (Eq. (1)), EVI (Eq. (2)), and SAVI (Eq. (3)) are derived using Red reflectance (Band 4 in Sentinel-2), Blue (Band 2) and Near-infrared (NIR) (Band 8). These indices are widely used to detect vegetation cover by leveraging the distinct way vegetation reflects and absorbs light.

$$NDVI = \frac{NIR - Red}{NIR + Red} \quad \text{(Eq. 1)}$$

$$EVI = 2.5 \times \frac{NIR - Red}{NIR + 6 \times Red - 7.5 \times Blue + 1} \quad \text{(Eq.2)}$$

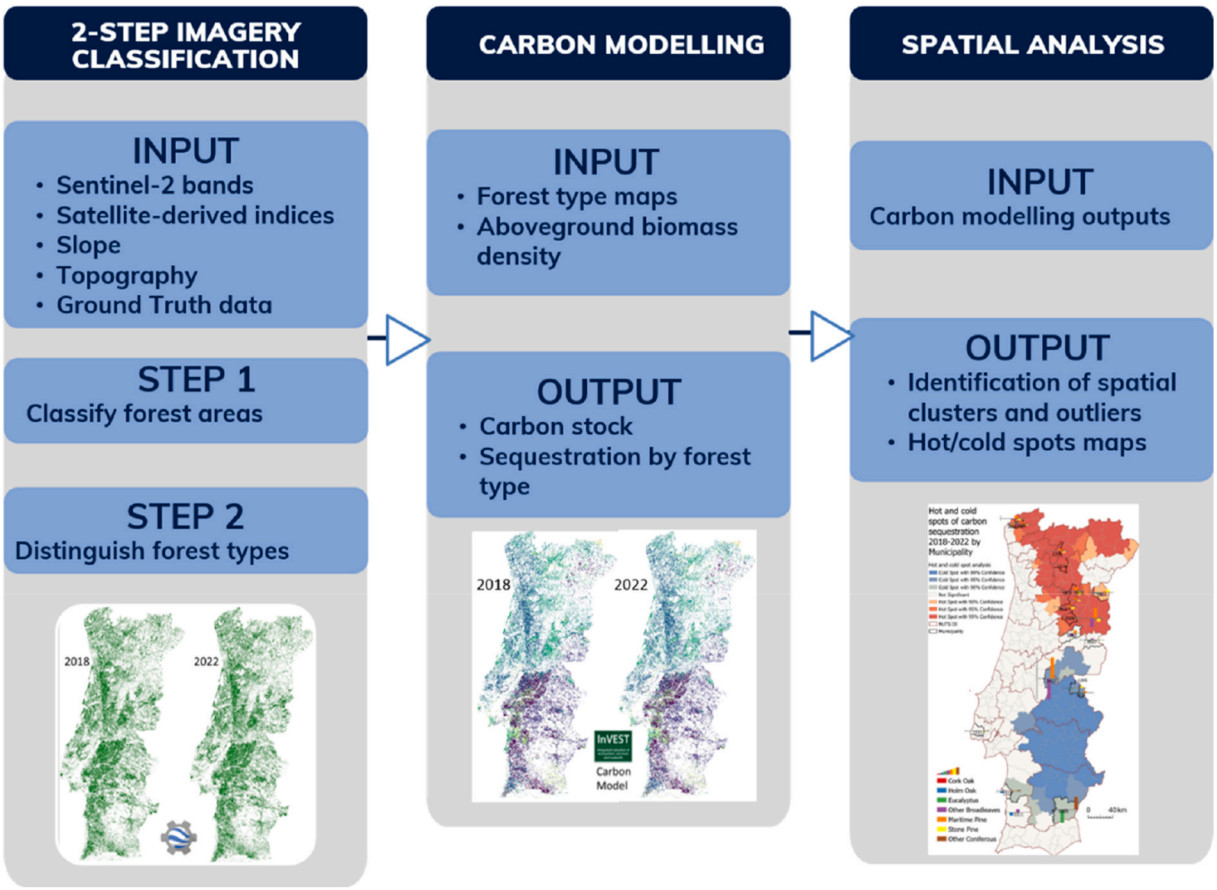

Fig. 2. Methodology schema illustrating the developed approach, which consists of: 1) Classifying forest and non-forest ecosystems and distinguishing forest types using binary and multiclass classification techniques; 2) Estimating carbon storage and sequestration (CSS); 3) Analyzing the relationships between forest types and potential carbon sequestration while mapping hot and cold spots of forest carbon distribution.

$$SAVI = \frac{(NIR - Red) \times (1 + L)}{NIR + Red + L} \quad \text{(Eq.3)}$$

The NDVI serves a proxy for vegetation density and health (Rouse et al., 1973) by measuring the difference between Red and NIR light reflectance. Red light is absorbed during photosynthesis, while NIR light is reflected by plant structures. The EVI is an improvement over NDVI, designed to minimize some of NDVI's limitations, particularly its sensitivity to atmospheric conditions (e.g., aerosols, haze) and soil reflectance (Huete et al., 1997). By incorporating correction factors and the Blue band, EVI accounts for atmospheric scattering and soil brightness, making it more responsive to changes in dense vegetation. The SAVI is another variation of NDVI, specifically designed to reduce the influence of soil brightness, making it particularly useful in areas with sparse vegetation where exposed soil is more visible prominent (Huete, 1988). It introduces a soil brightness correction factor, L, to adjust the vegetation index, thereby reducing the impact of bare soil. The commonly used value is L = 0.5 for intermediate vegetation cover. Table 1 lists the datasets used as input data in forest classification, CSS modelling, and result comparisons.

The reference data were obtained from the land use land cover map for the year 2018 (COS 2018), produced by the Directorate General for Territory (DGT, 2018), the national authority responsible for the environment and land administration of Portugal. Additionally, AGB density values for each forest class were compiled from the 6th Portuguese National Forestry Inventory, conducted in 2015 (ICNF, 2023). Table S1 (Supplementary Materials) provides a detailed list of forest classes and their respective AGB densities, measured in tonnes per hectare (tonnes/ha).

For validation and quality assessment, we conducted comparisons with other relevant datasets to enhance the contextual understanding of our results. Specifically, we utilized the Forest Type 2018 (10 m) dataset provided by the Copernicus Land Monitoring Service (2025) (CLMS), which classifies forests into four thematic categories: non-forest areas, broadleaved forest, Coniferous forest, and mixed zones. This allowed us to compare the total classified areas of Coniferous and broadleaved forests. Additionally, we compared our estimated total forested area with values from the Forest Resources Assessment (FRA) provided by FAO - UN (2020). To assess forest changes between 2018 and 2022, we cross-referenced our results with the Global Forest Change 2000–2023 dataset developed by Hansen et al. (2013).

2.2.2. *Cloud-based forest classification*

Several studies have employed SVM for similar applications and have compared its performance with other ML algorithms for mapping terrestrial ecosystems (Agrillo et al., 2021; Boutsoukis et al., 2019; Fang et al., 2023; Fitts et al., 2021; Monteiro et al., 2024; Sannigrahi et al., 2019b, 2019a; Tarantino et al., 2021; Y. Wang et al., 2021; M. Zhang et al., 2019). These studies benchmarked SVM

Table 1
Summary of datasets used for cloud-based classification in Google Earth Engine (GEE) and for Carbon Storage and Sequestration (CSS) modelling using the InVEST CSS model. The Role/Task column specifies whether a dataset was used as a predictor or target variable in a machine learning (ML) classification task or as an input variable in the carbon modelling.

Name	Source	Role/Task	Format	Spatial Resolution	Temporal Resolution
Harmonized Sentinel-2 MSI: MultiSpectral Instrument, Level-2A	Google Earth Engine (GEE) (https://developers.google.com/earth-engine/datasets/catalog/COPERNICUS_S2_SR_HARMONIZED)	Predictor/ML classification	Raster	10 m	2018 and 2022
Digital Surface Model (ALOS World 3D) Version 3.2 Japan Aerospace Exploration Agency (JAXA) – slope and elevation	GEE (https://developers.google.com/earth-engine/datasets/catalog/JAXA_ALOS_AW3D30_V3_2)	Predictor/ML classification	Raster	30 m	2021
Land use land cover map (COS 2018)	Directorate General for Territory (DGT) (https://geo2.dgterritorio.gov.pt/cos/COS2018/COS2018v2-shp.zip)	Target/ML classification	Vector	1 ha (Minimum mapping unit)	2018
Administrative limits (Country, NUTS III, Municipality)	DGT (https://www.dgterritorio.gov.pt/sites/default/files/ficheiros-cartografia/Cont_AAD_CAOP2022.zip)	Boundary demarcation	Vector	1:25,000	2022
6th Portuguese National Forestry Inventory	Institute for Forest and Nature Conservation (ICNF) (https://cdn.pefc.org/pefc.pt/media/2020-08/88597cd3-8e82-4bc6-aae6-fb66adb5303f/22eabe74-d55e-5246-bfec-15be43c3c1c9.pdf)	InVEST CSS model	Ground measurements	Value	2015
Forest Type 2018 - Copernicus Land Monitoring Services (CLMS)	https://land.copernicus.eu/en/products/high-resolution-layer-forest-type	Validation/ Comparison of results	Raster	10 m	2018
Global Forest Change 2000–2023 GE E Hansen et al. (2013)	https://glad.earthengine.app/view/global-forest-change	Validation/ Comparison of results	Raster	30 m	2018 to 2022
Global Forest Resources Assessment 2020 - Food and Agriculture Organization (FAO)	https://fra-data.fao.org/assessments/fra/2020/PRT/sections/extentOfForest	Validation/ Comparison of results	Values	–	2018

alongside Random Forest (RF) and deep learning (DL) models (Jagannathan and Divya, 2021; Pritt and Chern, 2018; Tarantino et al., 2021) and highlighted the high computational and time resources required by these approaches. Additionally, research by Sharma et al. (2018), S. Sannigrahi et al. (2019a), S. Sannigrahi et al. (2019b), Mouta et al. (2021) and Monteiro et al. (2024)compared SVM against four other ML algorithms. Their findings concluded that both SVM and RF produced the most accurate satellite-based classification predictions of forest type.

This study employs the SVM classifier for forest type classification, utilizing the GEE platform for its computational efficiency and robust ML capabilities. The GEE-SVM classifier is particularly well-suited for processing large-scale geospatial datasets and has been applied here to classify forest types based on Sentinel-2 imagery. To map national forest ecosystems, two classification tasks were conducted. The first task involved binary classification, mapping forest cover to create a mask for filtering out non-forest areas. The second task was a multiclass classification, distinguishing seven forest types. A total of 98,000 reference points were generated using a stratified random sampling approach, based on data from the COS2018 dataset. The SVM algorithm was applied to both classification tasks due to its robustness in handling complex datasets and its proven effectiveness in distinguishing forest features (Ghosh, 2014; Grabska et al., 2020; Shao and Lunetta, 2012; Suess et al., 2015).

The SVM classifier works by finding an optimal hyperplane that separates different classes within the feature space (Thanh Noi and Kappas, 2017). Its kernel-based approach makes it suitable for both linearly and non-linearly separable classes (Shao and Lunetta, 2012). However, the success of an SVM classification largely depends on selecting the appropriate kernel type, gamma, and cost parameters (Almeida et al., 2024). To determine the most suitable kernel and optimize gamma and cost parameters, a hyperparameter tuning method was implemented. The algorithm searched across different kernel types (linear, polynomial, radial basis function (RBF), and sigmoid), gamma values ranging from 0.1 to 10, and cost values between 1 and 100. These kernel functions allow SVM to handle various data patterns and relationships (Boser et al., 1992). As such, the linear kernel represents a linear decision boundary in the feature space; the polynomial type projects features into a higher-dimensional space using polynomial equations; the radial basis function measures the similarity between data points based on their distance, allowing for complex, non-linear decision boundaries; and the sigmoid kernel functions similarly to a neural network's activation function, mapping data into a non-linear space (Akiba et al., 2019). The gamma parameter controls the influence of individual training examples. Lower values create a broader area of influence, while higher values result in a more localized effect. The cost parameter determines the trade-off between correctly classifying training points and maintaining a smooth decision boundary. A higher cost forces the classifier to minimize misclassification errors, while a lower cost allows greater tolerance for errors, potentially improving generalization.

The performance of the classification tasks was evaluated using four key metrics: accuracy, precision, recall, and F1 score. These metrics are based on identifying the following classification outcomes: true positives (TP), which are the correctly predicted positive cases; true negatives (TN), as correctly classified non-forest pixels; false positives (FP), incorrectly predicted positive cases; and false negatives (FN) as pixels classified as non-forest when they are actually forest (Olofsson et al., 2013). Accuracy (Eq. (4)) is a class-independent metric that measures the overall correctness of the classification algorithm by calculating the proportion of correctly predicted instances. Precision (Eq. (5)) is the ratio of correctly predicted TP to the total predicted positives (TP + FP) indicating how reliable the positive predictions are. Recall (Eq. (6)) is the ratio of correctly predicted TP to the actual positives (TP + FN), assessing the model's ability to identify all relevant positive instances. F1 score (Eq. (7)) is the harmonic mean of precision and recall, making it particularly useful when dealing with imbalanced data or uneven class distributions.

$$Accuracy = \frac{TP + TN}{TP + TN + FP + FN} \quad \text{(Eq.4)}$$

$$Precision = \frac{TP}{TP + FP} \quad \text{(Eq.5)}$$

$$Recall = \frac{TP}{TP + FN} \quad \text{(Eq.6)}$$

$$F1\ score = 2 \times \frac{Precision \times Recall}{Precision + Recall} \quad \text{(Eq.7)}$$

For reproducibility, detailed GEE scripts, including hyperparameter tuning and classification workflows, are provided. The binary classification script is available at (https://code.earthengine.google.com/5a8a510d984c8090555daf08afbfc09d) and the multiclass classification script can be accessed at (https://code.earthengine.google.com/f5b1a9e8d50c82f0c93b66f10be9b724). Both workflows utilize Sentinel-2 imagery, spectral indices, and SVM algorithm for classification. The binary classification script distinguishes forest and non-forest areas, while the multiclass classification script further classifies forest areas into specific types. Accuracy validation, smoothing of results, and exportation of outputs for further analyzes are also included in the workflows.

2.2.3. InVEST CSS model

The forest type maps for 2018 and 2022, classified in the first stage, were used as inputs for the InVEST CSS model (version 3.14.2). This tool is designed to quantify CSS by modelling the amount of carbon stored within forest ecosystems. The model requires a raster map specifying forest types and a table detailing the AGB density (tonnes/ha) for each forest class.

Using this information, the model calculates the total carbon stored based on the extent of each forest type and simulates carbon sequestration changes over time. The outputs include carbon storage maps (raster format) at 10 m spatial resolution for the study years.

In these maps, the positive values indicate carbon sequestration, representing the amount of carbon absorbed, and the negative values indicate carbon loss, representing carbon that is not captured or released into the atmosphere. These outputs provide a detailed spatial representation of carbon dynamics, enabling a better understanding of forest carbon stocks and changes over time.

2.2.4. Spatial patterns analysis

Spatial statistical tests are generally classified into global and local statistics, each providing distinct insights into data distribution and the detection of significant spatial patterns (Ord and Getis, 2012). To assess spatial clustering, we applied the Global Moran's I statistic, which determines whether a spatial pattern is clustered, dispersed, or random. The Moran's I index ranges from −1 to 1, with positive values indicate a high degree of spatial correlation, while negative values suggest dispersion (Keith Ord and Getis, 2001). Once the global spatial autocorrelation structure was identified, we used Anselin's Local Moran''s I statistic to detect local clusters and outliers based on spatial autocorrelation. Additionally, the Getis-Ord Gi statistic was applied to classify municipalities into hot spots (areas with high carbon stocks) and cold spots (areas with lower carbon stocks). This analysis provides a finer-scale understanding of carbon distribution patterns.

To further explore spatial relationships, we computed Moran's Scatterplot, which helps assess how individual data points contribute to the global spatial autocorrelation, and assists in identifying potential outliers using standard regression diagnostics. The x-axis displays the z-transformed values of observations, expressed as deviations from the mean. The y-axis represents the row-standardized spatial weights matrix (W). The slope of the regression line fitted to this scatterplot corresponds to Moran's I, indicating the strength and direction of spatial autocorrelation. The scatterplot is divided into four quadrants, each representing a different type of spatial association. The lower left and upper right indicate spatial clustering, where similar values are located near each other, and the upper left and lower right represent spatial outliers, where values differ significantly from their neighboring observations, either low values surrounded by high values (low-high) or high values surrounded by low values (high-low).

A feature is considered part of a cluster if its Moran's I value is positive, indicating that it is surrounded by nearby features with similarly high or low attribute values. Conversely, a feature is classified as an outlier if its adjacent features have significantly different values, reflected by a negative Moran's I value. To evaluate the statistical significance of spatial clustering, the hot spot analysis computes the Getis-Ord Gi statistic along with a z-score and p-value. A high z-score and a small p-value indicate a cluster of high values (hot spot), and a low negative z-score and a small p-value indicate a cluster of low values (cold spot). The strength of the clustering effect increases as the z-score moves further from zero (either positively or negatively). If the z-score is close to zero, there is no significant spatial clustering.

In this context, a hot spot is identified by a positive Getis-Ord Gi value, while a cold spot corresponds to a negative value. It is important to note that these statistical results are reliable only when applied to datasets with more than 30 samples. Since this analysis is conducted at the municipality level, which includes 278 samples, these methods are well-suited for identifying meaningful spatial patterns.

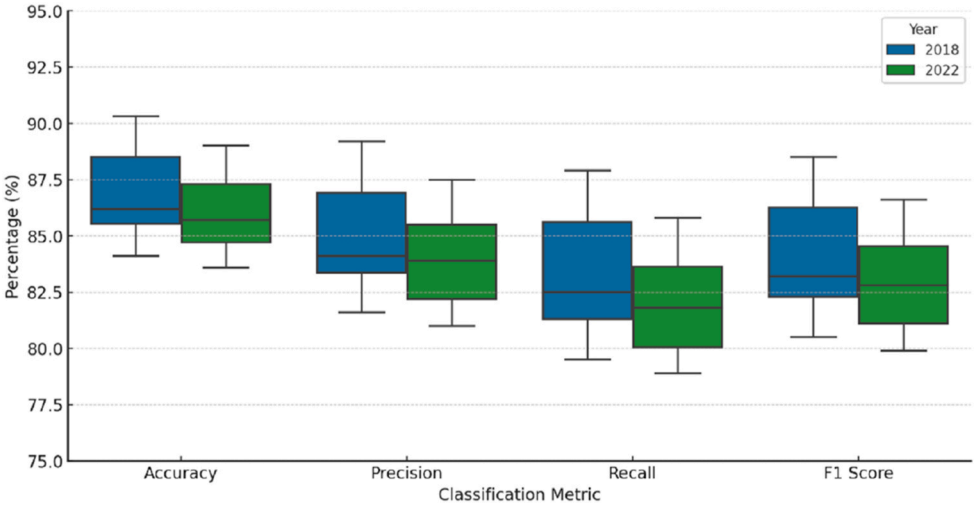

Fig. 3. Box plots illustrating the distribution of classification performance metrics (Accuracy, Precision, Recall, and F1 Score) for 2018 and 2022 across different forest types. The analysis distinguishes between Broadleaves (Quercus suber, Quercus ilex, *Eucalyptus* sp., and other species) and Coniferous (*Pinus pinaster*, Pinus pinea, and other species). For a detailed accuracy assessment and corresponding values for each class, please refer to Tables S2 and S3 in the Supplementary Materials.

3. Results

3.1. Forest ecosystems mapping

The classification outputs consist of four maps in raster format: two from binary classifications and two from multiclass classifications (Fig. S3 – Supplementary Materials). The tuning algorithm, implemented in both tasks, optimized classification accuracy by searching for the best combination of gamma, cost, and kernel functions. In both cases, the RBF kernel was selected. The optimal gamma values for the binary and multiclass tasks were 0.5 and 1.8, respectively, while the cost values were set at 10 and 60.

For forest/non-forest classification, the selected parameter values balanced accuracy, precision, and recall, resulting in a well-generalized model. For forest-type classification, the higher gamma and cost values produced more intricate decision boundaries. Overall, the SVM model performed better in classifying forest presence than in distinguishing specific forest types. The forest classification maps for 2018 and 2022 demonstrate high overall accuracy, with values of 92.2 % and 91 %, respectively. Although, there is a slight decrease in accuracy between these years, the results remain robust and reliable for analyzing spatiotemporal patterns of forest composition. The recall values were 91.8 % in 2018 and 90.5 % in 2022, showing a minor decrease over time. The precision values were 92 % in 2018 and 90.8 % in 2022, aligning closely with the recall values. The F1 score dropped slightly from 91.9 % in 2018 to 90.6 % in 2022, reflecting the overall trend of reduced accuracy, recall, and precision. This decline suggests that the classification performance in 2022 was slightly less effective in detecting forest areas compared to 2018. Possible reasons include: using ground truth data from 2018 to predict 2022; changes in environmental and atmospheric conditions between the two years; or variability in sensor data, which may have affected classification performance.

When distinguishing forest types within Broadleaves (Quercus suber, Quercus ilex, *Eucalyptus* sp., and other species), and Coniferous (*Pinus pinaster*, Pinus pinea, and other species), the accuracy values for all classes remain consistently high, exceeding 80 % in both years. However, a slight decline in accuracy is observed across most forest types from 2018 to 2022. The box plot (Fig. 3) provides a summary and comparison of classification performance metrics (Accuracy, Precision, Recall, and F1 Score) for 2018 and 2022 across forest types.

The Other Broadleaves class exhibits the highest accuracy in both years, with a slight decrease from 90.3 % in 2018 to 89 % in 2022. In contrast, the Other Coniferous category has the lowest accuracy, declining marginally from 84.1 % in 2018 to 83.6 % in 2022, suggesting greater difficulty in distinguishing this forest type. Precision values remain relatively stable but show a decline from 2018 to 2022 across all forest types. The Other Broadleaves class maintains the highest precision in both years (89.2 % in 2018 and 87.5 % in 2022), while the Other Coniferous and Stone Pine categories exhibit lower precision rates. *Eucalyptus* sp. And Other Broadleaves generally achieve higher recall rates, indicating that the model is good at detecting true positives for these forest types. However, there is a noticeable decline in recall for most forest types from 2018 to 2022, suggesting that the model has become slightly less effective in capturing all actual instances of the forest classes. The F1 score follows a similar trend, with a slight reduction across all classes from 2018 to 2022. The Other Broadleaves and Cork Oak categories maintain relatively high and stable F1 scores (86.6 % and 85.8 %, respectively), while the Other Coniferous class records the lowest F1 score (79.9 %), highlighting persistent challenges in achieving high precision and recall for this category.

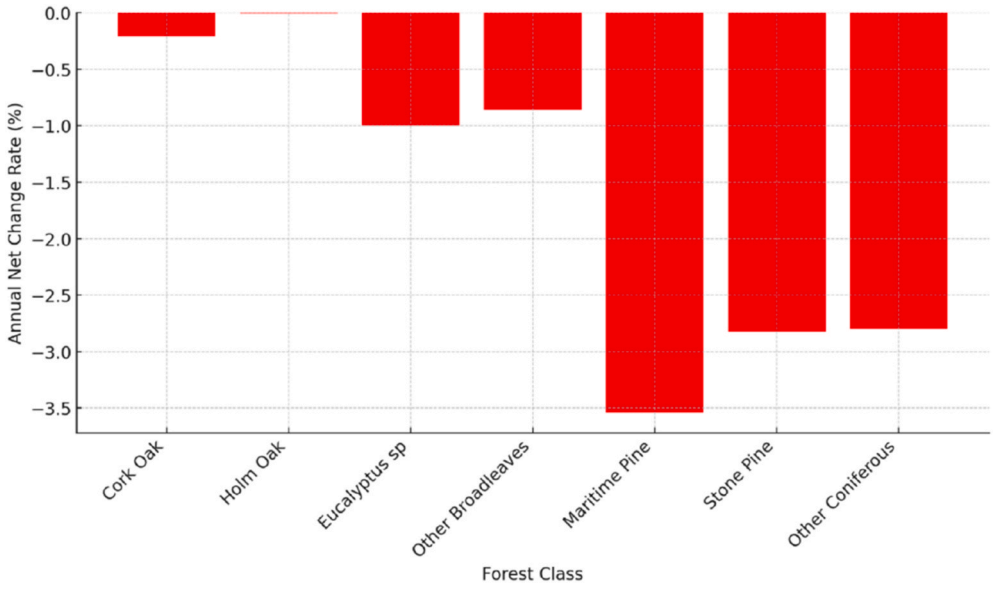

Fig. 4. Annual net change rate of forest area between reference years (2018–2022) grouped by forest classes.

3.2. National scale: assessing the SGD 15.2.1 indicators

The two SDG 15.2.1 indicators (1) annual net change rate of forest types (Fig. 4) and (2) AGB stock in forest ecosystems, were estimated at the national level, using 2018 and 2022 as reference years. The total forest extent in 2018 and 2022 were estimated in 2,711,427 ha and 2,579,482 ha, respectively, indicating a net reduction of 131,945 ha, with an annual loss rate of 26,389 ha/year. As a result, AGB carbon stock has also decreased, reducing the amount of carbon sequestered and stored. At the national level, Portugal experienced a decline in forest carbon sequestration of 0.22 tonnes/ha (220 kg/ha) between 2018 and 2022. This carbon loss is directly linked to the reduction in AGB, driven by negative net changes in total forest area over time.

Between 2018 and 2022, Portugal experienced an overall forest area decline with an annual net change rate of −1.22 %. Significant losses were observed in: *Eucalyptus* sp. (−1.00 %), Other Broadleaves (−0.86 %), Maritime Pine (−3.54 %), Stone Pine (−2.82 %), and Other Coniferous (−2.80 %). Among these, Maritime Pine suffered the highest decline. The largest absolute losses were observed in *Eucalyptus* sp. (−32,038 ha) and Maritime Pine (−63,423 ha). These trends indicate a progressive reduction in forest ecosystems, particularly among pine species, which may have implications for carbon storage, biodiversity, and ES.

3.3. Spatial patterns of forest CSS

3.3.1. Sub-regions (NUTS III)

Pearson's correlation was used to analyze the relationship between carbon storage and forest types at the NUTS III level for both years (Fig. S4 - Supplementary Materials). The results indicate a strong positive correlation between carbon storage and the Other Broadleaves, Other Coniferous and Stone Pine forest classes. In contrast, negative associations were observed with Holm Oak, Cork Oak, Maritime Pine and *Eucalyptus* sp. The heatmap (Fig. 5) illustrates differences in Pearson correlation coefficients between 2018 and 2022 for carbon storage and forest types. While most relationships remained stable, some notable shifts were observed, such as *Eucalyptus* sp. And Holm Oak showed decreasing correlations with carbon storage; and Maritime Pine and Other Coniferous exhibited increasing correlations with carbon storage. These changes suggest localized shifts in forest dynamics or carbon storage patterns over time.

To further understand these relationships, we analyzed carbon sequestration by forest type for each NUTS III sub-region (Fig. 6) between 2018 and 2022. The results indicate positive carbon stock in the northern and central sub-regions, while carbon losses were observed in Southern Portugal. Among the 23 sub-regions, six experienced a decline in carbon sequestration (184 - Baixo Alentejo, 150 - Algarve, 187 - Alentejo Central, 16H - Beira Baixa, 186 - Alto Alentejo, and 181 - Alentejo Litoral). In contrast, the remaining 17 sub-regions showed an increase in carbon capture over the same period.

Notably, the decline in carbon sequestration in these six sub-regions corresponds to a reduction in the area of Cork Oak and Holm Oak forests. The most pronounced Holm Oak losses were observed in regions 184 (Baixo Alentejo) and 16H (Beira Baixa), while Eucalyptus declines were most significant in regions 150 (Algarve) and 16H (Beira Baixa). This sub-regional analysis highlights carbon

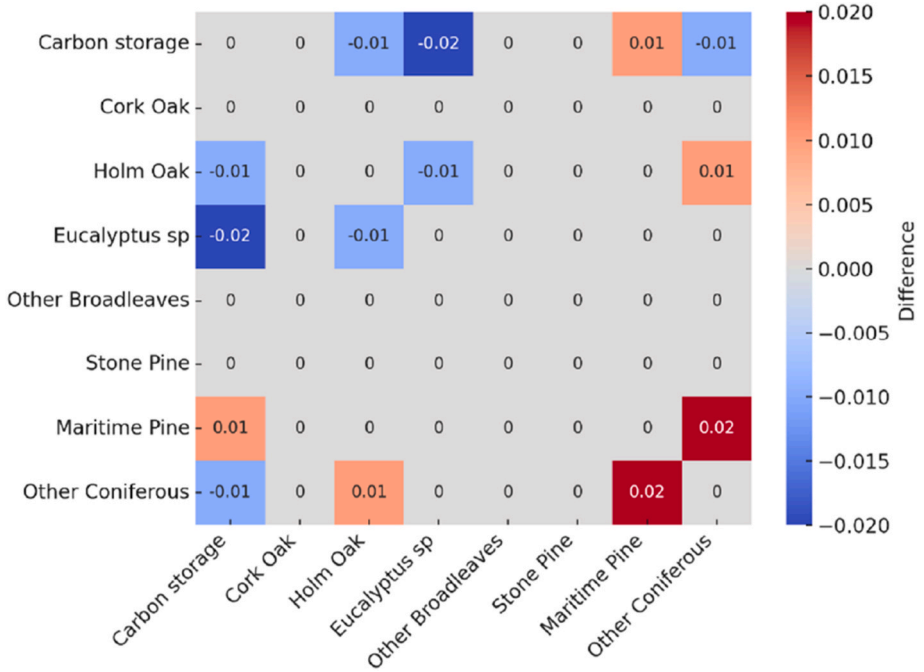

Fig. 5. Difference in Pearson's correlation between 2018 and 2022 within forest types and carbon storage.

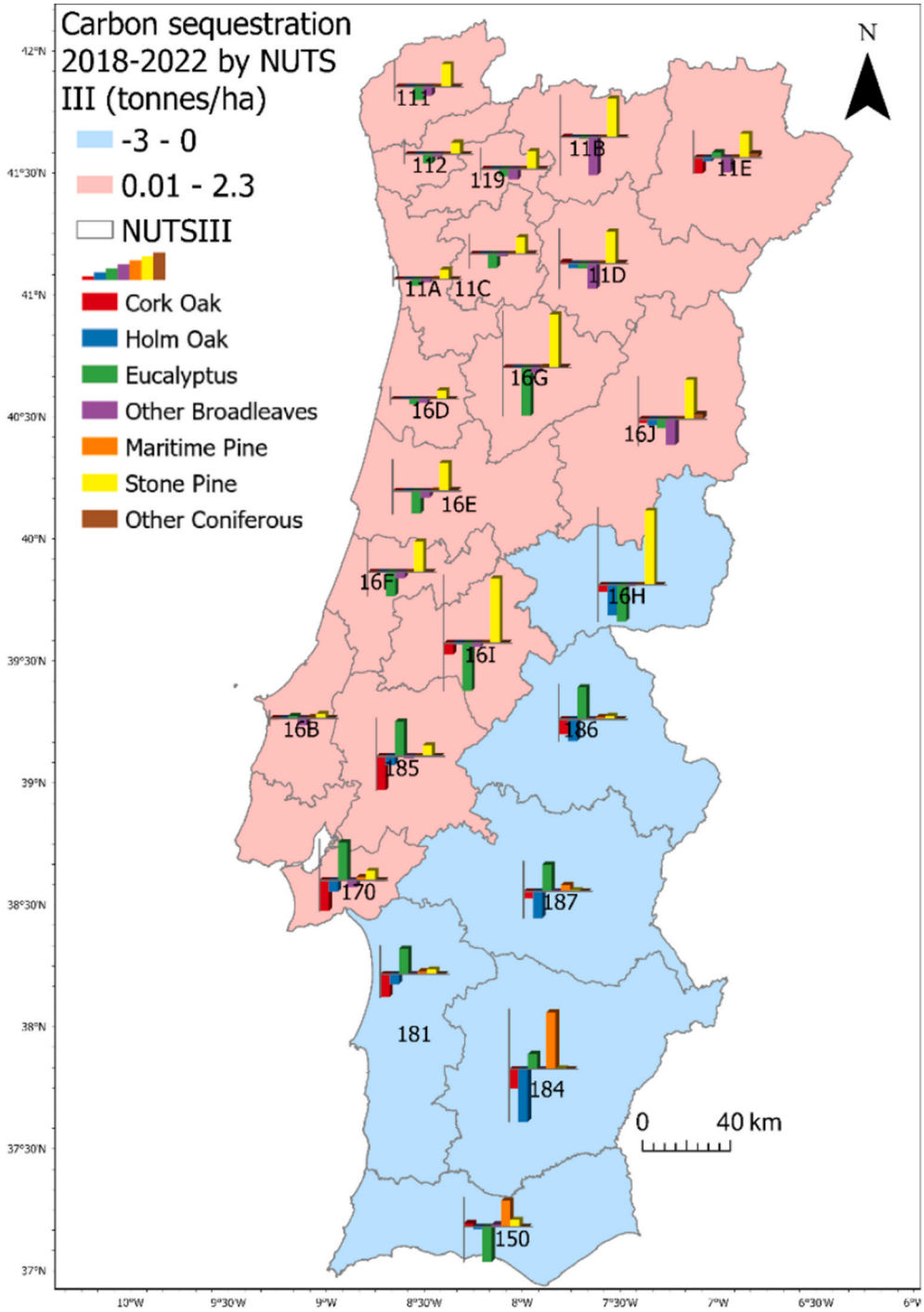

Fig. 6. Carbon sequestration (2018–2022) by forest by NUTS III (tonnes/ha). Legend: 11 B - Alto Tâmega; 11D – Douro; 16 J - Beiras e Serra da Estrela; 11 E - Terras de Trás-os-Montes; 119 - Ave; 111 - Alto Minho; 16 B – Oeste; 16 F - Região de Leiria; 16 E - Região de Coimbra; 170 - Área Metropolitana de Lisboa; 16D - Região de Aveiro; 16G - Viseu Dão Lafões; 11 A - Área Metropolitana do Porto; 16I - Médio Tejo; 11C - Tâmega e Sousa; 112 – Cávado; 185 - Lezíria do Tejo; 181 - Alentejo Litoral; 186 - Alto Alentejo; 16H - Beira Baixa; 187 - Alentejo Central; 150 – Algarve; 184 - Baixo Alentejo.

storage losses driven by changes in forest composition across NUTS III areas.

3.3.2. Municipalities

The Global Moran's I values are positive and statistically significant in both years, 0.67 in 2018 and 0.68 in 2022 (Table 2). The null hypothesis assumes that AGB carbon storage is randomly distributed among municipalities. However, since the p-values are statistically significant and z-scores are positive, there is less than a 1 % likelihood that this clustered pattern is due to random chance, leading to the rejection of the null hypothesis.

The first interpretation of local spatial patterns serves as a diagnostic tool for identifying outliers in relation to the global spatial association measure. While the overall spatial association is positive, as indicated by the slope of the regression line of the Moran's scatterplots (Fig. 7), four observations were identified as outliers in both years: (0901 - Aguiar da Beira, 0507 - Penamacor, 1205 - Castelo de Vide and 1210 - Marvão). In 2018, within the high-high cluster, one low-high outlier was identified in the upper left quadrant. Within the low-low cluster, two high-low outliers were located in the lower right quadrant. In 2022, two low-high outliers and one high-low outlier were identified.

Local Moran's I analysis identified local clusters of high–high values in 48 municipalities in northern Portugal in 2018, with one municipality flagged as a low-high spatial outlier (0901 - Aguiar da Beira). In the southern 44 municipalities were clustered by low-low carbon storage values, while two municipalities (1205 - Castelo de Vide and 1210 - Marvão) were classified as high-low outliers. By 2022, the number of high-high clustered municipalities in the north increased to 56, with two municipalities identified as low-high outliers (0901 - Aguiar da Beira and 0507 - Penamacor). In the south, 48 municipalities formed low-low clusters, with one high-low outlier (1210 - Marvão). Over time, 1205 - Castelo de Vide transitioned from a high-low outlier in 2018 to a low-low cluster in 2022, indicating a decline in carbon storage capacity. Meanwhile, 0507 -Penamacor, previously not statistically significant, became a low-high outlier, suggesting an increase in carbon potential. The mean carbon storage values in high-high clusters were 132.22 tonnes/ha in 2018 and 131.82 tonnes/ha in 2022. In low-low clusters, the mean values were 75.43 tonnes/ha in 2018 and 75.88 tonnes/ha in 2022. These results indicate a decrease in carbon storage in the northern region and an increase in the southern region from 2018 to 2022. A detailed statistical summary of these clustering changes over time is provided in Table 3.

The Getis–Ord Gi statistic was used to identify statistically significant clusters of high (hot spot) and low (cold spot) values of carbon sequestration over time (Fig. 8). At significance levels smaller than or equal to 10 %, results reveal hot spot clusters with high carbon sequestration in northern Portugal and cold spot clusters with low carbon sequestration in the south. In the north, the number of hot spot municipalities increased from 59 in 2018 to 60 in 2022. In the south, 50 municipalities were classified as cold spots in both years. The maps also highlight six municipalities that experienced changes in their grouping, either increasing or decreasing their likelihood of being clustered as cold or hot spots. In the north, the following municipalities increased their probability of being hot spots, shifting from hot 90 % to hot 95 % (0906 - Gouveia, 1709 - Ribeira de Pena, and 1818 – Sernancelhe). In the south, the following municipalities exhibited changes in their cold spot grouping: 0209 - Mértola shifted from cold 90 % to cold 95 %, increasing its likelihood of being a cod spot; 1413 - Mação changed from cold 95 % to cold 90 %, decreasing its likelihood of being clustered as a cod spot. Among these changes, 0503 - Covilhã stands out as the only municipality that transitioned from not significant to hot 90 %, indicating a notable increase in carbon sequestration potential. Fig. 8 illustrates these changes in forest type at the municipality between 2018 and 2022.

Mértola increased its likelihood of being clustered as a cold spot due to a 31,603 ha decrease in Maritime Pine forests. Conversely, Mação reduced its significance as a cold spot following a notable increase in forest area, particularly in *Eucalyptus* sp. (16,726 ha) and Other Broadleaves (211 ha), which have the highest carbon storage capacity.

Covilhã was the only municipality to transition from not statistically significant to a hot spot cluster, despite experiencing a loss of 10,566 of Other Broadleaves and 25,317 ha of Stone Pine forests. Similarly, Gouveia, Ribeira de Pena, and Sernancelhe increased their likelihood of being clustered as hot spots, despite a decline in forest area of Other Broadleaves and Stone Pine.

4. Discussion

This study advances the measurement of changes in CSS by developing an approach that integrates cloud-based satellite data acquisition and processing, open-source software for CSS modelling, and ESDA. This integrated methodology enables examining the relationship between AGB carbon storage and forest type, mapping clusters and outliers, and identifying hot and cold spots of carbon sequestration at the municipality level. The results highlight the importance of inter-annual assessments in understanding forest ecosystem' functioning at the national, NUTS III, and municipal scales.

4.1. Forest ecosystem mapping relied on satellite earth observation data and technologies

The integration of cloud computing for satellite imagery acquisition, processing, and analysis, combined with the InVEST CSS model, provided a robust framework for spatially explicit estimations of CSS in forest ecosystems. Forest mapping based on satellite

Table 2
Spatial autocorrelation confidence analysis using the Global Moran's I statistic across 278 municipalities.

Year	Moran's Index	Expected Index	Variance	z-score	p-value
2018	0.67	$-3.6*10^{-3}$	$7*10^{-4}$	23.83	0
2022	0.68	$-3.6*10^{-3}$	$7*10^{-4}$	24.23	0

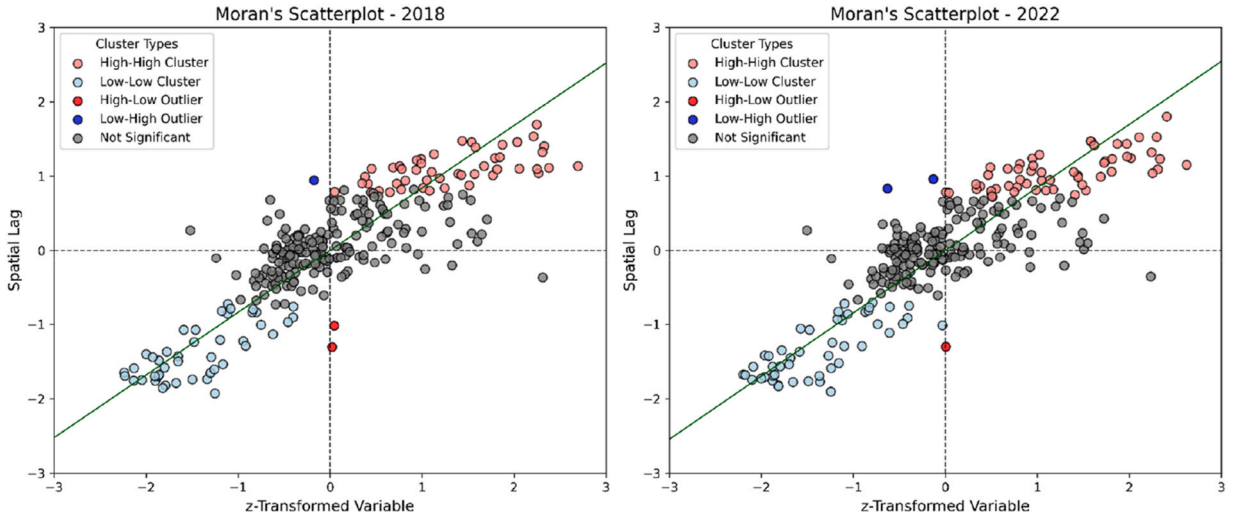

Fig. 7. Moran's scatterplots displaying the projection of all observations to visualize local instability in spatial autocorrelation. The x-axis represents the z-transformed vector of observations. The y-axis represents the row-standardized spatial weights matrix (W). The slope of the scatterplot corresponds to the linear regression of Wz on z, indicating the strength and direction of spatial autocorrelation. The scatterplot is divided into four quadrants each representing a different type of spatial association: lower left and upper right quadrants indicate spatial clustering of similar values (high-high or low-low), and upper left and lower right quadrants indicate spatial association of dissimilar values (outliers) (low-high or high-low).

Table 3
Descriptive statistics of carbon storage across all observations (278 municipalities) and within spatial clusters (HH: high-high, LL: low-low) for 2018 and 2022. The count column represents the number of municipalities included in each analysis.

Year	Mean	Median	Standard Deviation	Variance	Minimum	Maximum	Count
2018	104.87	102.50	20.74	4.30	58.56	160.63	278
2022	105.09	102.64	21.49	4.62	57.94	161.32	278
2018_HH	132.22	130.07	13.74	1.89	105.83	160.63	48
2022_HH	131.82	129.03	14.45	2.09	105.15	161.32	56
2018_LL	75.43	74.42	10.64	1.13	58.56	96.60	44
2022_LL	75.88	75.78	11.65	1.36	57.94	104.39	48

imagery not only highlighted carbon dynamics but also served as a crucial tool for informed decision-making in forest conservation and climate change mitigation strategies. The decision to use SVM as the classifier was guided by previous research comparing ML algorithms for mapping terrestrial ecosystems (Agrillo et al., 2021; Boutsoukis et al., 2019; Fang et al., 2023; Fitts et al., 2021; Monteiro et al., 2024; Sannigrahi et al., 2019b, 2019a; Tarantino et al., 2021; Y. Wang et al., 2021; M. Zhang et al., 2019). These studies identified SVM, along with RF and DL models, as leading classifiers (Jagannathan and Divya, 2021; Pritt and Chern, 2018; Tarantino et al., 2021), while also recognizing their high computational and time resource requirements. Moreover, Tarantino et al. (2021) argued that recent advancements in computing power, more efficient resource allocation, and the advent of cloud computing are helping to mitigate these limitations, making such models more accessible for large-scale analyses.

A limitation of this study is the temporal mismatch between data sources, including the reference dataset (COS, 2018), National Forest Inventory data (2015), and Sentinel-2 optical imagery (2018 and 2022). These discrepancies, arising from differences in the timing of data collection, may introduce uncertainties in the analysis and potentially affect the accuracy of trend detection. This limitation underscores the importance of harmonizing data collection efforts across sources in future studies to enhance the robustness and reliability of integrated methodologies. Acknowledging this challenge highlights the need for coordinated and consistent data acquisition to improve the precision of CSS assessments and spatial analyses. Noteworthy to remark is that the year 2018, following the catastrophic fires of 2017 in central Portugal, likely represents a period of forest regeneration especially for fast-growing species like *Eucalyptus* sp., which may influence our analysis. Similarly, we recognize that post-COVID-19 effects on habitat suitability during and after 2022, as highlighted by Sil et al. (2017), could also play a role.

Detailed forest-cover classification on a broad scale is technically constrained by the difficulty of distinguishing forest classes with similar spectral signatures. The subtle spectral similarities between certain forest types can lead to confusion and misclassification, as the model may struggle to generalize when there is a significant overlap in the spectral characteristics of different classes (Gwal et al., 2020). By focusing exclusively on forested pixels identified in the first classification phase, the multiclass classification achieved a more targeted and accurate mapping of forest types, improving overall accuracy and reducing false positives. Additionally, the effectiveness of the SVM algorithm depended on both hyperparameter settings (Monteiro et al., 2024) which were automatically optimized, and the quality of the input data (Khwarahm, 2021). The overall performance for both years suggests a balanced trade-off

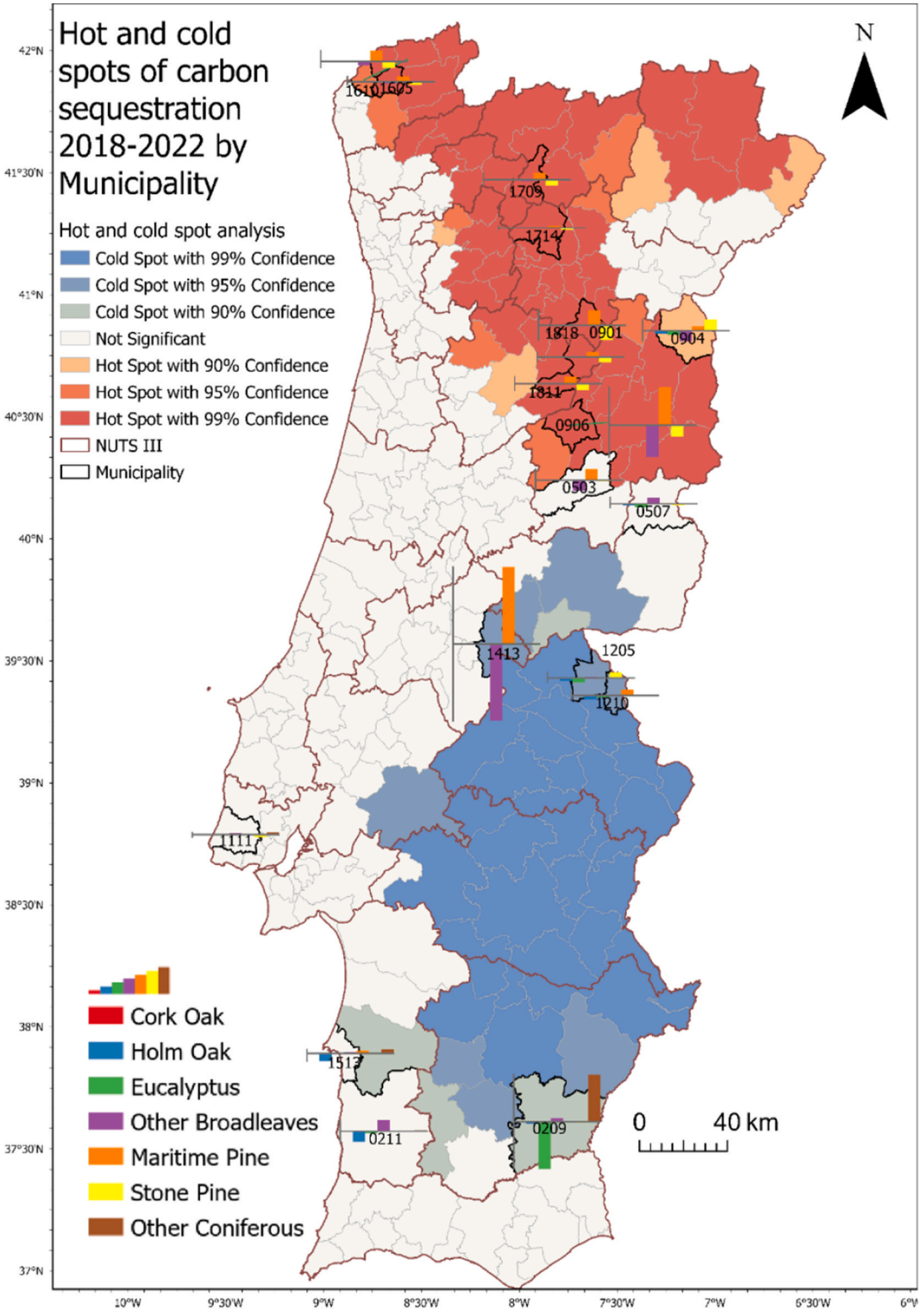

Fig. 8. Hot and cold spot analysis of carbon sequestration between 2018 and 2022 and the 18 flagged municipalities identified in the Getis–Ord Gi statistics. Legend: 0209 – Mértola; 0211 – Odemira; 0503 – Covilhã; 0507 – Penamacor; 0901 - Aguiar da Beira; 0904 - Figueira de Castelo Rodrigo; 0906 – Gouveia; 1111 – Sintra; 1205 - Castelo de Vide; 1210 – Marvão; 1413 – Mação; 1513 – Sines; 1610 - Vila Nova de Cerveira; 1709 - Ribeira de Pena; 1714 - Vila Real, 1811 - Penalva do Castelo, 1818 – Sernancelhe; 1605 - Paredes de Coura.

between precision and recall, though slightly higher precision is needed to ensure that identified forest classes are classified correctly. While the model performed better in general forest classification, the added complexity of forest-type classification was justified by the need to differentiate among more nuanced classes. Although the SVM classifier was effective in both tasks, further hyperparameter refinement is recommended to improve classification quality. A cross-validation strategy combined with hyperparameters optimization could help maximize accuracy, precision, and recall while avoiding overfitting. Additionally, integrating climatic datasets could enhance the model, enabling the generation of climate-driven forest classification maps.

For validation and quality assessment, several datasets were used as references to compare our results including: FRA from FAO - UN (2020), the Global Maps of 21st-Century Forest Cover Change (GFC) developed by Hansen et al. (2013), and the Forest type dataset provided by Copernicus Land Monitoring Service (2025). The FRA estimates a total forest extent of 3,312,000 ha, while our classification reports a lower value of 2,711,427 ha, resulting in a difference of 600,573 ha (18.13 %). The Forest type dataset estimates 2, 352,440 ha of broadleaved forests and 552,248 ha of Coniferous forests, whereas our classification reports 2,106,195 ha and 605,232 ha, respectively. Compared to CMLS, our results show 10.47 % less broadleaved area and 9.59 % more Coniferous area. The GFC dataset estimates 107,019 ha of forest loss, while our classification reports 131,945 ha, a 23.3 % higher loss. This discrepancy is likely due to differences in methodology, spatial resolution, and forest definitions. Our Sentinel-2-based classification may capture finer-scale changes that the Landsat-based GFC approach does not detect. These comparisons underscore the importance of harmonizing classification criteria and using multiple datasets to improve assessment reliability.

Between 2018 and 2022, Portugal's mainland lost 131,945 ha of forested area, implying a forest loss rate of 26,389 ha/year. The annual national report of forest fires (ICNF, 2023) recorded 136,511 ha of forest loss due to rural fires, i.e. 20,626 ha in 2018; 21,163 ha in 2019; 31,803 ha in 2020; 8118 ha in 2021; and 54,801 ha in 2022. Comparing these values with the total forest area change (131, 945 ha) and the annual mean loss rate (26,389 ha/year), our results are underestimated by 3.34 %. Similarly, Cunha et al. (2021) observed an underestimation when analyzing intervention scenarios using the InVEST CSS at the regional scale. Their research highlighted a limitation of the model in simplifying the Earth's carbon cycle and assuming a linear change in carbon storage over time. Nevertheless, such models provide valuable proxies for supporting nature conservation, resource management, policymaking, and landscape planning.

We employed widely recognized vegetation indices (NDVI, EVI, and SAVI) derived from Sentinel-2 imagery to monitor vegetation health, density, and soil-vegetation interactions. However, indices derived from MODIS data, such as Leaf Area Index (LAI) and the fraction of photosynthetically active radiation (FPAR), offer valuable insights into canopy structure and photosynthetic activity, in addition to providing long-term temporal coverage, making them ideal for broad-scale and long-term analyses. Compared to MODIS, which has a coarser resolution (250 m - 1 km), Sentinel-2 enables a more detailed examination of spatial heterogeneity in forest landscapes at municipal and sub-regional levels. Future research could explore integrating LAI and FPAR with Sentinel-2 data, and combining multiple remote sensing platforms to gain a more comprehensive understanding of vegetation dynamics and their influence on carbon fluxes. A data fusion approach could bridge the gap between spatial detail and physiological complexity, further enhancing CSS assessments.

4.2. Spatial patterns analysis of forest carbon stock

This study employed modelling techniques and spatial statistics to support forest carbon sequestration enhancement through strategic land-use planning and management. The study timeframe of 2018 and 2022 was selected primarily due to the availability of compatible reference datasets provided by national authorities. The five-year interval was intentionally chosen to assess the methodology's ability to capture meaningful trends over a relatively short period, particularly in relation to changes in forest type area and their influence on CSS variability. While we recognize the limitations of comparing only two years, this approach allowed us to validate the robustness of our method in detecting changes in forest type distribution and carbon storage, while also highlighting forest types as key drivers of CSS variability. Additionally, uncertainties arising from the COS2018 dataset, particularly for mixed forest systems like Quercus suber, introduce challenges in accurately distinguishing dominant species. These ambiguities may impact species-specific classification and, consequently, carbon modelling accuracy.

The global and local analyses provided insights into carbon storage distribution at the national level, identifying patterns, clusters, and variations at the local level. Since many existing tools provide information at scales too coarse for managers to effectively use (Gaur and Simonovic, 2019), our approach offers detailed insights that support informed decision-making and environmental problem-solving at multiple administrative levels. While we acknowledge the limitations of administrative boundaries, which may not always align with ecological scales, these units remain necessary for studying socioeconomic and environmental interdependencies. The results highlight the importance of analyzing the inter-annual variations at country, NUTS III and municipal levels, advancing the understanding of the forest ecosystem functioning and demonstrating how carbon magnitude and distribution are directly influenced tree type distribution.

The cold and hot spots clusters of forest carbon storage reflect global differences in socio-environmental conditions, including human activities such as deforestation, logging, land conversion, landscape management, climate, water availability, topography, and soil, which heavily influence the spatial distribution of forest CSS (Y Wang et al., 2021). Focusing on the environmental aspects, the North of Portugal flagged as a hotspot of forest carbon is characterized by higher water availability, precipitation, and evapotranspiration (Almeida and Cabral, 2021) providing means for more dense canopies and high biodiversity. Unlikely, the southern region (cold spot) is more vulnerable to extreme weather events such as droughts that can weaken trees, making them more susceptible to pests and diseases, and wildfires, which can cause significant changes in forest structure and composition. By identifying regions with high and low carbon stocks, forest managers can target specific areas for conservation, restoration, and climate change mitigation

efforts. These insights support sustainable forest management practices that optimize carbon sequestration and enhance the resilience of forest ecosystems.

4.3. Monitoring progress towards sustainable forest management

Monitoring and managing forest carbon are critical components of global efforts to combat climate change, preserve biodiversity, and promote environmental sustainability (Keith et al., 2021b). SDG indicator 15.2.1 encompasses multiple aspects of sustainable forest management, serving as a key measure of forest health, vitality, and ecosystem benefits (Estoque, 2020). Assessing forest conditions through metrics such as carbon stock, species richness, and habitat diversity provides valuable insights into forest degradation, species variety and abundance, and the resilience of forests in supporting ecological processes at both national and local scales. These assessments enable monitoring national progress towards sustainable forest management and allow comparisons with countries and regions. Furthermore, they provide evidence-based data to support policymakers in taking informed decisions for strategic land-use planning and forest conservation.

The methodology developed supports forest management by providing a systematic and comprehensive record of CSS, which can be applied to any other carbon pools. Additionally, it helps address critical questions related to the current distribution and quantity of carbon stored and/or sequestered at various spatial scales (national, catchment, municipal, or land parcel levels). For instance, the carbon opportunity cost of land conversions, helping to assess trade-offs between different land-use decisions; map carbon sinks and sources to identify areas of high carbon sequestration and loss; identify the economic and social values provided by forest ecosystems, supporting sustainable development policies.

4.4. Recommendations for enhancing forest carbon sequestration

Portugal's forests are heavily dominated by monocultures, particularly *Eucalyptus* sp. Plantations, which cover vast areas of the landscape. While these fast-growing species are economically significant, their prevalence reduces biodiversity, increases fire susceptibility, and limits ecosystem resilience. The lack of diverse forest mosaics, consisting of a mix of species and land uses, is a direct consequence of historical land-use practices, socioeconomic shifts, and rural depopulation. Promoting the development of forest mosaics through reforestation with native species and sustainable land-use planning is critical for enhancing resilience and restoring ES. Addressing these structural challenges requires policies that incentivize active forest management, support rural revitalization, and balance ecological sustainability with economic needs.

There are several recommendations and practices that can help countries mitigate climate change and achieve SDG. One key strategy is prioritized land-use management, which involves understanding forest carbon dynamics and determining carbon opportunity costs across different forest species (Korosuo et al., 2023). Such studies provide valuable insights into opportunities for land use conversion, evaluation of direct and indirect benefits and costs, quantification of long-term and passive gains, comparison of net present values (Han et al., 2022). In the context of forest management, opportunity cost analysis is essential for making informed decisions that balance ecological, economic, and social benefits (Navarro et al., 2017). Since different forest species exhibit varying capacities for carbon sequestration, analyzing trade-offs within forest types is a valuable tool for sustainable decision-making. The benefits and costs of different forest management strategies can be represented by provisioning capacity of forest-derived products (timber, resins, nuts) and ES such as water and climate regulation, soil erosion control, and biodiversity conservation. Therefore, economic evaluations of goods and services associated with each forest type should be integrated into land use comparisons. These evaluations should not only consider forest alternatives but also other land uses including agriculture, urban development, and industrial activities such as clean energy production and mining.

Beyond protecting existing forests from deforestation and degradation, maintaining carbon storage capacity and enhancing resilience to climate change and other stressors is essential. An adaptive management strategy should 1) anticipate and respond to changing climate conditions, including wildfires, pests, and disease outbreaks; 2) establish protection efforts for vulnerable ecosystems; 3) develop and implement policies to prevent illegal logging and land conversion; 4) engage local communities by providing incentives and alternative livelihoods to support sustainable forest management. Continuous carbon stock and flux monitoring in forests, using remote sensing and ground-based measurements, is critical for understanding carbon dynamics across different forest types and management practices. Additionally, policies and financial incentives should be developed and promoted to encourage society, landowners and stakeholders to adopt measures that optimize CSS.

5. Conclusions

Using Satellite Earth Observation data and technologies, this study analyzes the spatial distribution of carbon sequestration across seven forest types, offering valuable insights for Portugal's efforts to efficiently manage carbon resources; actively reduce GHG emissions; combat climate change through forest conservation and monitoring; and mitigate desertification and land degradation, and biodiversity loss. It establishes baseline data to support land-use conversion decisions by examining the relationships between forest type and carbon stock, and highlights that the granularity of analysis is a crucial factor, particularly for regional and local planning purposes. Moreover, this approach enables furthering the assessment of the values and services provided by forest ecosystems, including provisioning services (wood and non-wood products), regulating services (climate and water regulation, sediment retention), and cultural services (recreational opportunities).

CRediT authorship contribution statement

Bruna Almeida: Writing – review & editing, Writing – original draft, Methodology, Investigation, Formal analysis, Data curation, Conceptualization. **Luís Monteiro:** Writing – review & editing, Methodology, Conceptualization, Formal analysis. **Rafaela Tiengo:** Writing – review & editing, Formal analysis. **Artur Gil:** Writing – review & editing, Methodology, Conceptualization. **Pedro Cabral:** Writing – review & editing, Methodology, Conceptualization, Project administration.

Ethical Statement

Hereby, I Bruna Almeida, consciously assure that for the manuscript "Spatially explicit assessment of carbon storage and sequestration in forest ecosystems".

1) This material is the authors' own original work, which has not been previously published elsewhere.
2) The paper is not currently being considered for publication elsewhere.
3) The paper reflects the authors' own research and analysis in a truthful and complete manner.
4) The paper properly credits the meaningful contributions of co-authors and co-researchers.
5) The results are appropriately placed in the context of prior and existing research.
6) All sources used are properly disclosed (correct citation). Literally copying of text must be indicated as such by using quotation marks and giving proper references.
7) All authors have been personally and actively involved in substantial work leading to the paper and will take public responsibility for its content.

I agree with the above statements and declare that this submission follows the policies of Remote Sensing Applications: Society and Environment as outlined in the Guide for Authors and in the Ethical Statement.

Declaration of competing interest

The authors declare that they have no known competing financial interests or personal relationships that could have appeared to influence the work reported in this paper.

Acknowledgements

This work was supported by the research project MaSOT – Mapping Ecosystem Services from Earth Observations, funded by the Portuguese Science Foundation – FCT [EXPL/CTA-AMB/0165/2021], and by national funds through FCT (Fundação para a Ciência e a Tecnologia), under the project - UIDB/04152/2020 (DOI: 10.54499/UIDB/04152/2020) - Centro de Investigação em Gestão de Informação (MagIC)/NOVA IMS). We are grateful to the anonymous reviewers for their comments and recommendations which improved the manuscript.

Appendix A. Supplementary data

Supplementary data to this article can be found online at https://doi.org/10.1016/j.rsase.2025.101544.

Data availability

Data will be made available on request.

References

Agrillo, E., Filipponi, F., Pezzarossa, A., Casella, L., Smiraglia, D., Orasi, A., Attorre, F., Taramelli, A., 2021. Earth observation and biodiversity big data for forest habitat types classification and mapping. Remote Sens. 13, 1231. https://doi.org/10.3390/rs13071231.

Akiba, T., Sano, S., Yanase, T., Ohta, T., Koyama, M., 2019. Optuna: a next-generation hyperparameter optimization framework. In: Proceedings of the 25th ACM SIGKDD International Conference on Knowledge Discovery & Data Mining, KDD '19. Association for Computing Machinery, New York, NY, USA, pp. 2623–2631. https://doi.org/10.1145/3292500.3330701.

Almeida, B., Cabral, P., 2021. Water yield modelling, sensitivity analysis and validation: a study for Portugal. ISPRS Int. J. GeoInf. 10. https://doi.org/10.3390/ijgi10080494.

Almeida, B., David, J., Campos, F.S., Cabral, P., 2024. Satellite-based machine learning modelling of ecosystem services indicators: a review and meta-analysis. Appl. Geogr. https://doi.org/10.1016/j.apgeog.2024.103249.

Anselin, L., 1995. Local indicators of spatial association—lisa. Geogr. Anal. 27, 93–115. https://doi.org/10.1111/J.1538-4632.1995.TB00338.X.

Araya, Y.H., Cabral, P., 2010. Analysis and modeling of urban land cover change in Setúbal and Sesimbra, Portugal. Remote Sens. 2, 1549–1563. https://doi.org/10.3390/rs2061549.

Boser, B.E., Guyon, I.M., Vapnik, V.N., 1992. A training algorithm for optimal margin classifiers. In: Proceedings of the Fifth Annual Workshop on Computational Learning Theory, pp. 144–152.

Boutsoukis, C., Manakos, I., Heurich, M., Delopoulos, A., 2019. Canopy height estimation from single multispectral 2D airborne imagery using texture analysis and machine learning in structurally rich temperate forests. Remote Sens. 11, 2853. https://doi.org/10.3390/rs11232853.

Bui, M., Adjiman, C.S., Bardow, A., Anthony, E.J., Boston, A., Brown, S., Fennell, P.S., Fuss, S., Galindo, A., Hackett, L.A., Hallett, J.P., Herzog, H.J., Jackson, G., Kemper, J., Krevor, S., Maitland, G.C., Matuszewski, M., Metcalfe, I.S., Petit, C., Puxty, G., Reimer, J., Reiner, D.M., Rubin, E.S., Scott, S.A., Shah, N., Smit, B., Trusler, J.P.M., Webley, P., Wilcox, J., Dowell, N. Mac, 2018. Carbon capture and storage (CCS): the way forward. Energy Environ. Sci. 11, 1062. https://doi.org/10.1039/c7ee02342a.

Chen, G., Singh, K.K., Lopez, J., Zhou, Y., 2020. Tree canopy cover and carbon density are different proxy indicators for assessing the relationship between forest structure and urban socio-ecological conditions. Ecol. Indic. 113, 106279. https://doi.org/10.1016/J.ECOLIND.2020.106279.

Coelho, M.F., Ramos, A., de Lima, I., Trigo, R., 2013. Seasonal changes in daily precipitation extremes in mainland Portugal from 1941 to 2007. Reg. Environ. Change 14. https://doi.org/10.1007/s10113-013-0515-6.

Cong, C., Pan, H., Page, J., Barthel, S., Kalantari, Z., 2023. Modeling place-based nature-based solutions to promote urban carbon neutrality. Ambio 52, 1297–1313. https://doi.org/10.1007/S13280-023-01872-X/FIGURES/3.

Copernicus Land Monitoring Service, 2025. Copernicus Land Monitoring Service.

Cunha, J., Campos, F.S., David, J., Padmanaban, R., Cabral, P., 2021. Carbon sequestration scenarios in Portugal: which way to go forward? Environ. Monit. Assess. 193, 1–14. https://doi.org/10.1007/S10661-021-09336-Z/FIGURES/7.

David, J., Cabral, P., Campos, F.S., 2024. Humans versus models: a comparative assessment of ecosystem services models and stakeholders' perceptions. Sci. Rep. 14, 25995. https://doi.org/10.1038/s41598-024-76600-w.

DGT, 2018. Technical Specifications of the Land Use and Land Cover Map for Portugal Mainland [WWW Document]. URL (accessed 8.3.23.

Ermitão, T., Páscoa, P., Trigo, I., Alonso, C., Gouveia, C., 2023. Mapping the most susceptible regions to fire in Portugal. Fire 6. https://doi.org/10.3390/FIRE6070254, 2023, Page 254 6, 254.

ESRI, 2023. ArcGIS Pro - ESRI. Environmental Systems Research Institute.

Estoque, R.C., 2020. A review of the sustainability concept and the state of SDG monitoring using remote sensing. Remote Sens. 12. https://doi.org/10.3390/rs12111770.

Eurostat, 2023. Database - population and demography [WWW Document]. URL. https://ec.europa.eu/eurostat/web/population-demography/demography-population-stock-balance/database, 1.17.23.

Fang, P., Ou, G., Li, R., Wang, L., Xu, W., Dai, Q., Huang, X., 2023. Regionalized classification of stand tree species in mountainous forests by fusing advanced classifiers and ecological niche model. GIsci Remote Sens 60. https://doi.org/10.1080/15481603.2023.2211881.

FAO - UN, 2020b. Global Forest Resources Assessment 2020 - FRA Platform.

Fedrigo, M., Kasel, S., Bennett, L.T., Roxburgh, S.H., Nitschke, C.R., 2014. Carbon stocks in temperate forests of south-eastern Australia reflect large tree distribution and edaphic conditions. Ecol. Manag. 334, 129–143. https://doi.org/10.1016/J.FORECO.2014.08.025.

Fitts, L.A., Russell, M.B., Domke, G.M., Knight, J.K., 2021. Modeling land use change and forest carbon stock changes in temperate forests in the United States. Carbon Bal. Manag. 16, 20. https://doi.org/10.1186/s13021-021-00183-6.

Fonseca, F., de Figueiredo, T., Vilela, Â., Santos, R., de Carvalho, A.L., Almeida, E., Nunes, L., 2019. Impact of tree species replacement on carbon stocks in a Mediterranean mountain area, NE Portugal. Ecol. Manag. 439, 181–188. https://doi.org/10.1016/j.foreco.2019.03.002.

Gaur, A., Simonovic, S.P., 2019. Introduction to physical scaling: a model aimed to bridge the gap between statistical and dynamic downscaling approaches. Trends and Changes in Hydroclimatic Variables: Links to Climate Variability and Change 199–273. https://doi.org/10.1016/B978-0-12-810985-4.00004-9.

Getis, A., Ord, J.K., 1992. The analysis of spatial association by use of distance statistics. Geogr. Anal. 24, 189–206. https://doi.org/10.1111/J.1538-4632.1992.TB00261.X.

Ghosh, S., 2014. A tutorial on different classification techniques for remotely sensed imagery datasets. The Smart Computing Review 4. https://doi.org/10.6029/smartcr.2014.01.004.

Goetz, S.J., Baccini, A., Laporte, N.T., Johns, T., Walker, W., Kellndorfer, J., Houghton, R.A., Sun, M., 2009. Mapping and monitoring carbon stocks with satellite observations: a comparison of methods. Carbon Bal. Manag. 4, 2. https://doi.org/10.1186/1750-0680-4-2.

Google, 2023. Google earth engine [WWW Document]. URL. https://earthengine.google.com/, 9.5.23.

Gorelick, N., Hancher, M., Dixon, M., Ilyushchenko, S., Thau, D., Moore, R., 2017. Google earth engine: planetary-scale geospatial analysis for everyone. Remote Sens. Environ. 202, 18–27. https://doi.org/10.1016/j.rse.2017.06.031.

Grabska, E., Frantz, D., Ostapowicz, K., 2020. Evaluation of machine learning algorithms for forest stand species mapping using Sentinel-2 imagery and environmental data in the Polish Carpathians. Remote Sens. Environ. 251, 112103. https://doi.org/10.1016/J.RSE.2020.112103.

Gwal, S., Singh, S., Gupta, S., Anand, S., 2020. Understanding forest biomass and net primary productivity in Himalayan ecosystem using geospatial approach. Model Earth Syst Environ 6, 2517–2534. https://doi.org/10.1007/s40808-020-00844-4.

Han, J., Hu, Z., Mao, Z., Li, G., Liu, S., Yuan, D., Guo, J., 2022. How to account for changes in carbon storage from coal mining and reclamation in eastern China? Taking yanzhou coalfield as an example to simulate and estimate. Remote Sens. 14, 2014. https://doi.org/10.3390/rs14092014.

Hansen, M.C., Potapov, P.V., Moore, R., Hancher, M., Turubanova, S.A., Tyukavina, A., Thau, D., Stehman, S.V., Goetz, S.J., Loveland, T.R., Kommareddy, A., Egorov, A., Chini, L., Justice, C.O., Townshend, J.R.G., 2013. High-resolution global maps of 21st-century forest cover change. Science 342, 850–853. https://doi.org/10.1126/science.1244693, 1979.

Holzwarth, S., Thonfeld, F., Abdullahi, S., Asam, S., Da Ponte Canova, E., Gessner, U., Huth, J., Kraus, T., Leutner, B., Kuenzer, C., 2020. Earth observation based monitoring of forests in Germany: a review. Remote Sens. 12, 3570. https://doi.org/10.3390/rs12213570.

Hossain, M.S., Hashim, M., 2019. Potential of Earth Observation (EO) technologies for seagrass ecosystem service assessments. Int. J. Appl. Earth Obs. Geoinf. 77, 15–29. https://doi.org/10.1016/J.JAG.2018.12.009.

Houghton, R.A., Hall, F., Goetz, S.J., 2009. Importance of biomass in the global carbon cycle. J Geophys Res Biogeosci 114. https://doi.org/10.1029/2009JG000935.

Hudak, A.T., Fekety, P.A., Kane, V.R., Kennedy, R.E., Filippelli, S.K., Falkowski, M.J., Tinkham, W.T., Smith, A.M.S., Crookston, N.L., Domke, G.M., Corrao, M.V., Bright, B.C., Churchill, D.J., Gould, P.J., McGaughey, R.J., Kane, J.T., Dong, J., 2020. A carbon monitoring system for mapping regional, annual aboveground biomass across the northwestern USA. Environ. Res. Lett. 15, 95003. https://doi.org/10.1088/1748-9326/ab93f9.

Huete, A.R., 1988. A soil-adjusted vegetation index (SAVI). Remote Sens. Environ. 25, 295–309. https://doi.org/10.1016/0034-4257(88)90106-X.

Huete, A.R., Liu, H.Q., van Leeuwen, W.J.D., 1997. Use of vegetation indices in forested regions: issues of linearity and saturation. International Geoscience and Remote Sensing Symposium (IGARSS) 4, 1966–1968. https://doi.org/10.1109/IGARSS.1997.609169.

ICNF, 2023. Instituto da Conservação da Natureza e das Florestas [WWW Document]. URL. https://sig.icnf.pt/portal/home/, 1.24.23.

Islam, I., Cui, S., Hoque, M.Z., Abdullah, H.M., Tonny, K.F., Ahmed, M., Ferdush, J., Xu, L., Ding, S., 2022. Dynamics of tree outside forest land cover development and ecosystem carbon storage change in eastern coastal zone, Bangladesh. Land 11, 76. https://doi.org/10.3390/land11010076.

Jagannathan, J., Divya, C., 2021. Deep learning for the prediction and classification of land use and land cover changes using deep convolutional neural network. Ecol. Inform. 65, 101412. https://doi.org/10.1016/J.ECOINF.2021.101412.

Jiang, F., Sun, H., Ma, K., Fu, L., Tang, J., 2022. Improving aboveground biomass estimation of natural forests on the Tibetan Plateau using spaceborne LiDAR and machine learning algorithms. Ecol. Indic. 143, 109365. https://doi.org/10.1016/J.ECOLIND.2022.109365.

Keith, H., Vardon, M., Obst, C., Young, V., Houghton, R., Mackey, B., 2021a. Evaluating nature-based solutions for climate mitigation and conservation requires comprehensive carbon accounting. Sci. Total Environ. 769, 144341. https://doi.org/10.1016/j.scitotenv.2020.144341.

Keith, H., Vardon, M., Obst, C., Young, V., Houghton, R., Mackey, B., 2021b. Evaluating nature-based solutions for climate mitigation and conservation requires comprehensive carbon accounting. Sci. Total Environ. 769, 144341. https://doi.org/10.1016/j.scitotenv.2020.144341.

Keith Ord, J., Getis, A., 2001. Testing for local spatial autocorrelation in the presence of global autocorrelation. J. Reg. Sci. 41, 411–432. https://doi.org/10.1111/0022-4146.00224.

Khwarahm, N.R., 2021. Spatial modeling of land use and land cover change in Sulaimani, Iraq, using multitemporal satellite data. Environ. Monit. Assess. 193. https://doi.org/10.1007/s10661-021-08959-6.
King, S., Agra, R., Zolyomi, A., Keith, H., Nicholson, E., de Lamo, X., Portela, R., Obst, C., Alam, M., Honzák, M., Valbuena, R., Nunes, P.A.L.D., Santos-Martin, F., Equihua, M., Pérez-Maqueo, O., Javorsek, M., Alfieri, A., Brown, C., 2024. Using the system of environmental-economic accounting ecosystem accounting for policy: a case study on forest ecosystems. Environ. Sci. Pol. 152, 103653. https://doi.org/10.1016/J.ENVSCI.2023.103653.
Korosuo, A., Pilli, R., Abad Viñas, R., Blujdea, V.N.B., Colditz, R.R., Fiorese, G., Rossi, S., Vizzarri, M., Grassi, G., 2023. The role of forests in the EU climate policy: are we on the right track? Carbon Bal. Manag. 18, 15. https://doi.org/10.1186/s13021-023-00234-0.
Kumar, L., Mutanga, O., 2018. Google earth engine applications since inception: usage, trends, and potential. Remote Sens. 10. https://doi.org/10.3390/rs10101509.
Lade, S.J., Steffen, W., de Vries, W., Carpenter, S.R., Donges, J.F., Gerten, D., Hoff, H., Newbold, T., Richardson, K., Rockström, J., 2020. Human impacts on planetary boundaries amplified by Earth system interactions. Nat. Sustain. 3, 119–128. https://doi.org/10.1038/s41893-019-0454-4.
Li, X., 2023. Big earth data boost UN SDGs. Sci Bull (Beijing) 68, 773–774. https://doi.org/10.1016/J.SCIB.2023.03.045.
Li, H., Hiroshima, T., Li, X., Hayashi, M., Kato, T., 2024. High-resolution mapping of forest structure and carbon stock using multi-source remote sensing data in Japan. Remote Sens. Environ. 312. https://doi.org/10.1016/j.rse.2024.114322.
Li, Y., Yuan, L., Song, Z., Yu, S., Zhang, X., Tian, B., Liu, M., 2024. Salt marsh carbon stock estimation using deep learning with Sentinel-1 SAR of the Yangtze River estuary, China. Int. J. Appl. Earth Obs. Geoinf. 133, 104138. https://doi.org/10.1016/J.JAG.2024.104138.
Manley, K., Nyelele, C., Egoh, B.N., 2022. A review of machine learning and big data applications in addressing ecosystem service research gaps. Ecosyst. Serv. 57, 101478. https://doi.org/10.1016/J.ECOSER.2022.101478.
Matsala, M., Myroniuk, V., Bilous, A., Terentiev, A., Diachuk, P., Zadorozhniuk, R., 2020. An indirect approach to predict deadwood biomass in forests of Ukrainian Polissya using Landsat images and terrestrial data. For. Stud. 73, 107–124. https://doi.org/10.2478/fsmu-2020-0018.
Meddens, A.J.H., Steen-Adams, M.M., Hudak, A.T., Mauro, F., Byassee, P.M., Strunk, J., 2022. Specifying geospatial data product characteristics for forest and fuel management applications. Environ. Res. Lett. 17. https://doi.org/10.1088/1748-9326/ac5ee0.
Moran, P.A.P., 1950. A test for the serial independence of residuals. Biometrika 37, 178–181. https://doi.org/10.1093/biomet/37.1-2.178.
Mouta, N., Silva, R., Pais, S., Alonso, J.M., Gonçalves, J.F., Honrado, J., Vicente, J.R., 2021. 'The best of two worlds'—combining classifier fusion and ecological models to map and explain landscape invasion by an alien shrub. Remote Sens. 13. https://doi.org/10.3390/rs13163287.
Naidoo, L., van Deventer, H., Ramoelo, A., Mathieu, R., Nondlazi, B., Gangat, R., 2019. Estimating above ground biomass as an indicator of carbon storage in vegetated wetlands of the grassland biome of South Africa. Int. J. Appl. Earth Obs. Geoinf. 78, 118–129. https://doi.org/10.1016/J.JAG.2019.01.021.
Narine, L.L., Popescu, S.C., Malambo, L., 2019. Synergy of ICESat-2 and landsat for mapping forest aboveground biomass with deep learning. Remote Sens. 11, 1503. https://doi.org/10.3390/rs11121503.
Carbon | Natural Capital Project, 2023.
Navarro, J.A., 2017. First experiences with google earth engine. In: Proceedings of the 3rd International Conference on Geographical Information Systems Theory, Applications and Management - GISTAM. SciTePress, pp. 250–255. https://doi.org/10.5220/0006352702500255.
Navarro, L.M., Fernández, N., Guerra, C., Guralnick, R., Kissling, W.D., Londoño, M.C., Muller-Karger, F., Turak, E., Balvanera, P., Costello, M.J., Delavaud, A., El Serafy, G.Y., Ferrier, S., Geijzendorffer, I., Geller, G.N., Jetz, W., Kim, E.S., Kim, H.J., Martin, C.S., McGeoch, M.A., Mwampamba, T.H., Nel, J.L., Nicholson, E., Pettorelli, N., Schaepman, M.E., Skidmore, A., Sousa Pinto, I., Vergara, S., Vihervaara, P., Xu, H., Yahara, T., Gill, M., Pereira, H.M., 2017. Monitoring biodiversity change through effective global coordination. Curr. Opin. Environ. Sustain. 29, 158–169. https://doi.org/10.1016/J.COSUST.2018.02.005.
Nelson, E., Mendoza, G., Regetz, J., Polasky, S., Tallis, H., Cameron, Dr, Chan, K.M.A., Daily, G.C., Goldstein, J., Kareiva, P.M., Lonsdorf, E., Naidoo, R., Ricketts, T.H., Shaw, Mr, 2009. Modeling multiple ecosystem services, biodiversity conservation, commodity production, and tradeoffs at landscape scales. Front. Ecol. Environ. 7, 4–11. https://doi.org/10.1890/080023.
Nowak, D.J., Ellis, A., Greenfield, E.J., 2022. The disparity in tree cover and ecosystem service values among redlining classes in the United States. Landsc. Urban Plann. 221. https://doi.org/10.1016/j.landurbplan.2022.104370.
Olofsson, P., Foody, G.M., Stehman, S.V., Woodcock, C.E., 2013. Making better use of accuracy data in land change studies: estimating accuracy and area and quantifying uncertainty using stratified estimation. Remote Sens. Environ. 129, 122–131. https://doi.org/10.1016/J.RSE.2012.10.031.
Ord, J.K., Getis, A., 2012. Local spatial heteroscedasticity (LOSH). Ann. Reg. Sci. 48, 529–539. https://doi.org/10.1007/S00168-011-0492-Y/METRICS.
Pan, H., Page, J., Shi, R., Cong, C., Cai, Z., Barthel, S., Thollander, P., Colding, J., Kalantari, Z., 2023. Contribution of prioritized urban nature-based solutions allocation to carbon neutrality. Nat. Clim. Change 13 (8 13), 862–870. https://doi.org/10.1038/s41558-023-01737-x, 2023.
Paul, Keryn I., Roxburgh, S.H., England, J.R., 2022. Sequestration of carbon in commercial plantations and farm forestry. Trees, Forests and People 9, 100284. https://doi.org/10.1016/J.TFP.2022.100284.
Pérez-Cutillas, P., Pérez-Navarro, A., Conesa-García, C., Zema, D.A., Amado-Álvarez, J.P., 2023. What is going on within google earth engine? A systematic review and meta-analysis. Remote Sens. Appl. 29, 100907. https://doi.org/10.1016/J.RSASE.2022.100907.
Polasky, S., Nelson, E., Pennington, D., Johnson, K.A., 2011. The impact of land-use change on ecosystem services, biodiversity and returns to landowners: a case study in the state of Minnesota. Environ. Resour. Econ. 48, 219–242. https://doi.org/10.1007/s10640-010-9407-0.
Pritt, M., Chern, G., 2018. Satellite image classification with deep learning. Proceedings - Applied Imagery Pattern Recognition Workshop 2017-Octob, pp. 4–10. https://doi.org/10.1109/AIPR.2017.8457969.
Qasim, M., Csaplovics, E., 2023. Comparative study of forest biomass and carbon stocks of Margalla Hills National Park, Pakistan. For. Sci. Technol. 19, 139–154. https://doi.org/10.1080/21580103.2023.2208141.
Ramos, A.M., Russo, A., DaCamara, C.C., Nunes, S., Sousa, P., Soares, P.M.M., Lima, M.M., Hurduc, A., Trigo, R.M., 2023. The compound event that triggered the destructive fires of October 2017 in Portugal. iScience 26. https://doi.org/10.1016/j.isci.2023.106141.
Rogers, D., Setzler, B., Chiu, Y.W., 2019. Using plant functional groups as a strategy for modeling carbon dynamics in grassland ecosystems. Adv Environ Stud 3, 191–197.
Rouse, J., Haas, R., Schell, J., Deering, D., 1973. Monitoring vegetation systems in the great plains with ERTS. Third ERTS Symposium. NASA.
Sannigrahi, S., Chakraborti, S., Joshi, P.K., Keesstra, S., Sen, S., Paul, S.K., Kreuter, U., Sutton, P.C., Jha, S., Dang, K.B., 2019a. Ecosystem service value assessment of a natural reserve region for strengthening protection and conservation. J. Environ. Manag. 244, 208–227. https://doi.org/10.1016/j.jenvman.2019.04.095.
Sannigrahi, S., Joshi, P.K., Keesstra, S., Paul, S.K., Sen, S., Roy, P.S., Chakraborti, S., Bhatt, S., 2019b. Evaluating landscape capacity to provide spatially explicit valued ecosystem services for sustainable coastal resource management. Ocean Coast Manag. 182, 104918. https://doi.org/10.1016/j.ocecoaman.2019.104918.
Santos, F.L.M., Couto, F.T., Dias, S.S., Ribeiro, N.A., Salgado, R., 2023a. Vegetation fuel characterization using machine learning approach over southern Portugal. Remote Sens. Appl., 101017 https://doi.org/10.1016/J.RSASE.2023.101017.
Santos, F.L.M., Couto, F.T., Dias, S.S., Ribeiro, N. de A., Salgado, R., 2023b. Vegetation fuel characterization using machine learning approach over southern Portugal. Remote Sens. Appl. 32, 101017. https://doi.org/10.1016/j.rsase.2023.101017.
Shao, Y., Lunetta, R.S., 2012. Comparison of support vector machine, neural network, and CART algorithms for the land-cover classification using limited training data points. ISPRS J. Photogrammetry Remote Sens. 70, 78–87. https://doi.org/10.1016/J.ISPRSJPRS.2012.04.001.
Sharma, A., Hubert-Moy, L., Buvaneshwari, S., Sekhar, M., Ruiz, L., Bandyopadhyay, S., Corgne, S., 2018. Irrigation history estimation using multitemporal landsat satellite images: application to an intensive groundwater irrigated agricultural watershed in India. Remote Sens. 10, 893. https://doi.org/10.3390/rs10060893.
Sil, Â., Fonseca, F., Gonçalves, J., Honrado, J., Marta-Pedroso, C., Alonso, J., Ramos, M., Azevedo, J.C., 2017. Analysing carbon sequestration and storage dynamics in a changing mountain landscape in Portugal: insights for management and planning. Int J Biodivers Sci Ecosyst Serv Manag 13, 82–104. https://doi.org/10.1080/21513732.2017.1297331.
Spawn, S.A., Sullivan, C.C., Lark, T.J., Gibbs, H.K., 2020. Harmonized global maps of above and belowground biomass carbon density in the year 2010. Sci. Data 7, 1–22. https://doi.org/10.1038/s41597-020-0444-4, 2020, 1 7.
Suess, S., Van Der Linden, S., Okujeni, A., Leitão, P.J., Schwieder, M., Hostert, P., 2015. Using class probabilities to map gradual transitions in shrub vegetation from simulated EnMAP data. Remote Sens. 7, 10668–10688. https://doi.org/10.3390/RS70810668, 2015, 10668-10688 7.

Tarantino, C., Forte, L., Blonda, P., Vicario, S., Tomaselli, V., Beierkuhnlein, C., Adamo, M., 2021. Intra-annual sentinel-2 time-series supporting grassland habitat discrimination. Remote Sens. 13, 1–29. https://doi.org/10.3390/rs13020277.

Thanh Noi, P., Kappas, M., 2017. Comparison of random forest, k-nearest neighbor, and support vector machine classifiers for land cover classification using sentinel-2 imagery. Sensors 18. https://doi.org/10.3390/S18010018. Page 18 18, 18, 2018.

Tiengo, R., Pacheco, J., Uchôa, J., Gil, A., 2021. Using Sentinel-1 GRD SAR Data for Volcanic Eruptions Monitoring: the Case-Study of Fogo Volcano (Cabo Verde) in 2014/2015.

Tiengo, R., Merino-De-Miguel, S., Uchôa, J., Gil, A., 2024. A land cover change detection approach to assess the effectiveness of conservation projects: a study case on the EU-funded life projects in são miguel island, azores (2002–2021). Land 13. https://doi.org/10.3390/land13050666.

United Nations, 2023. Goal 15: life on land - the global goals [WWW document]. URL. https://www.globalgoals.org/goals/15-life-on-land/, 8.7.23.

Wang, Y., Zhang, X., Peng, P., 2021. Spatio-temporal changes of land-use/land cover change and the effects on ecosystem service values in Derong county, China, from 1992-2018. Sustainability 13, 1–16. https://doi.org/10.3390/su13020827.

Wentling, C., Campos, F.S., David, J., Cabral, P., 2021. Pollination potential in Portugal: leveraging an ecosystem service for sustainable agricultural productivity. Land 10. https://doi.org/10.3390/land10040431.

Zhang, J., Okin, G.S., Zhou, B., 2019. Assimilating optical satellite remote sensing images and field data to predict surface indicators in the Western U.S.: assessing error in satellite predictions based on large geographical datasets with the use of machine learning. Remote Sens. Environ. 233, 111382. https://doi.org/10.1016/j.rse.2019.111382.

Zhang, M., Du, H., Zhou, G., Li, X., Mao, F., Dong, L., Zheng, J., Liu, H., Huang, Z., He, S., 2019. Estimating forest aboveground carbon storage in Hang-Jia-Hu using landsat TM/OLI data and random forest model. Forests 10, 1004. https://doi.org/10.3390/f10111004.